Chem Soc Rev

Fluorescence Sensing Systems for Gold and Silver Species

Journal:	*Chemical Society Reviews*
Manuscript ID:	CS-REV-09-2014-000328.R1
Article Type:	Review Article
Date Submitted by the Author:	30-Sep-2014
Complete List of Authors:	Singha, Subhankar; Pohang University of Science and Technology, Department of Chemistry Kim, Dokyoung; POSTECH, Seo, Hyewon; Pohang University of Science and Technology, Department of Chemistry Cho, Seo Won; Pohang University of Science and Technology, Department of Chemistry Ahn, Kyo Han; Pohang University of Science and Technology, Department of Chemistry

Chem Soc Rev

RSCPublishing

REVIEW ARTICLE

Fluorescence Sensing Systems for Gold and Silver Species

Cite this: DOI: 10.1039/x0xx00000x

Subhankar Singha,†[a] Dokyoung Kim,†[a] Hyewon Seo,[a] Seo Won Cho,[a] and Kyo Han Ahn*[a]

Received 00th October 2014,
Accepted 00th October 2014

DOI: 10.1039/x0xx00000x

www.rsc.org/

Besides the noble physical appearance of gold and silver, their novel chemical properties attracted the modern technology for various industrial, chemical and biological usages including the medical applications. The widespread use of gold and silver, however, can causes potential hazards to our environment. Therefore, suitable detection methods are prerequisite for evaluation of the harmful effects as well as for studying of their beneficial biological properties. Due to the several advantages over the conventional analytical methods, the fluorescence detection of gold and silver has become an active research area in the recent years. In this review, we overviewed the reported fluorescent detection systems for gold and silver species, and discussed their sensing properties with promising features. The future scopes of developments in this field of research are also mentioned.

1. Introduction

Noble metals that are resistant to corrosion and oxidation in moist air include gold, silver, ruthenium, rhodium, osmium, iridium, platinum and palladium. Among those, gold and silver have fascinated mankind since the earliest days of technological innovation, due to their lustrous appearance, malleability and noble characters, being used in currency coins, jewelry and ornaments, high-value tableware and utensils. Besides the physical appearance, gold and silver possess several unique chemical properties, which attracted the recent attention of their use for various purposes including chemical and biological applications. The widespread use of gold and silver, however, can cause adverse effects to the environment as well as in biological systems. Accordingly, suitable detection methods are required for evaluation of the adverse effects as well as for investigating their beneficial biological effects. The conventional analytical methods for gold and silver species are mostly useful for *ex vivo* analysis but pose certain limitations for *in vivo* analysis. For the latter purpose, small-molecular fluorescence sensing systems offer tools of choice.

In this review, we briefly introduced chemical properties and biological utilities of gold and silver species separately, followed by a short discussion on the conventional detection systems and the advantages of the fluorescence detection methods. The main part of this review is focused on the reported fluorescence detection systems for gold and silver species, which are discussed with their sensing properties. Some unique approaches of colorimetric detection systems are also included.

2. Gold

2.1. Gold species

2.1.1. Chemical properties

Gold (Au) is a group 11 transition metal in the periodic table, with the atomic number 79. Chemically, gold is one of the least reactive chemical elements and can possess several oxidation states: commonly 0, +1, and +3 and rarely −1, +2, +4, and +5 states.[1]

Au(I) complexes have the electron configuration of $[Xe]4f_{14}5d_{10}$ and usually form linear compounds with sp hybridization at gold. For example, AuCl, a commercially available source of Au(I), exists as a polymeric chain with μ-Cl ligands. AuCl is stable to air and moisture, but can undergo reduction to Au(0) slowly along with formation of $Au^{III}_2Cl_6$. Au(I) shows soft metal ion character, which prefers the soft donor atom such as sulfur and phosphine over hard atoms such as nitrogen and oxygen.[2,3] Au(III) complexes have electron configuration of $[Xe]4f_{14}d_8$ and usually show square planar structures with four ligands. Au(III) is a hard metal ion and thus favors hard donor atom such as nitrogen and oxygen, in contrast to Au(I). $AuCl_3$, a commercially available source of Au(III), exists as a dimer (Au_2Cl_6) with μ-Cl ligands. The cheapest commercial source of Au(III) is $MAuCl_4 \cdot 2H_2O$ (M = Na or K), which can be prepared from chlorauric acid ($HAuCl_4$),

which, in turn, prepared from metallic gold by oxidizing with chlorine or with aqua regia.[4]

Additionally, gold has nuclear spin of 3/2, but because of a very low sensitivity and a quadrupole moment, only a few ^{79}Au spectra in a highly symmetric environment have been reported. However, the diamagnetic character of both Au(I) and Au(III) allows the monitoring of catalysis reactions by NMR.[5]

Gold and its complexes are fascinating metal species widely used in catalysis, surface chemistry, materials and theoretical investigations. Au shows the strongest relativistic effect among related transition metal elements.[6,7] Thus, Au has 6s orbitals contracted whereas 5d orbitals expanded. Both Au(III) and cationic Au(I) species hence show superior Lewis acidity, in particular toward alkynes, activating them toward nucleophilic addition. The strong alkynophilicity of gold complexes has been explored in various chemical transformations. Since the seminal report by Teles *et al.* in 1998 that cationic Au(I)-phosphine complexes catalyzed hydration of alkynes,[8] a "gold-rush" begun in homogenous catalysis, leading to discovery of many types of new chemical transformations.[9–11]

Along with the gold-rush in searching for chemical conversions catalyzed or promoted by gold species, gold nanoparticles below 5 nm size or so have been exploited for the chemical reactions on the surface.[12] Furthermore, gold nanoparticles (AuNPs) of ≤100 nm size have received tremendous attention in various fields including chemistry, biology, and clinical chemistry, for their advantageous chemical and photophysical properties given by the large surface-to-volume ratio, high stability in the light or biological media, and tunable photophysical properties that can be readily tuned by surface modifications.[13]

2.1.2. Biological utilities

Au(I) complexes have long been used to treat rheumatoid arthritis.[14] They are known to inhibit protein tyrosine phosphatases (PTPs), presumably through reversible binding to the active site cysteine reside.[15] Soft Au(I) complexes readily coordinate to soft sulfur and phosphorous donor atoms. Those of gold–thiol complexes such as solganol, auranofin and sanocrysin are representative gold-based drugs for the treatment of several disease including asthma, malaria, HIV, and brain lesions (Fig. 1).[16–18]

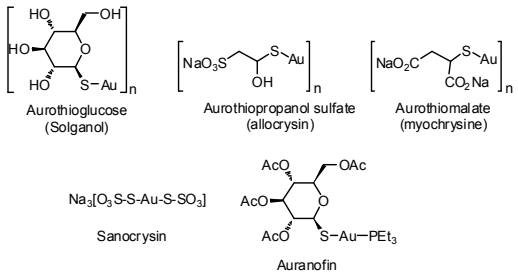

Fig. 1 Au(I)-thiolate drugs used for rheumatoid arthritis.

Au(III) is isoelectronic with platinum(II) and forms square planar complexes in general. After the discovery of cisplatin, platinum anticancer complexes have been extensively investigated, leading to several anticancer drugs.[19,20] Research activity on other organometallic therapeutic agents has led to investigation of gold complexes as anticancer agents. Despite the interesting medicinal properties of gold ions, their soluble salts such as gold chloride are known to cause damages to the liver, kidneys, and the peripheral nervous systems. Some Au(III) complexes are known to tightly bind certain enzymes, DNA or other biomolecules, disturbing a variety of cellular processes.[21–24]

Recently, Au(I) species coupled with organic fluorophores also have been utilized for bioimaging purpose to find out potential drug candidates. In general, Au(I) complexes have broad physiologically therapeutic value,[25] whereas Au(III) complexes show toxic effects to the biosystems.[26] In the reducing cellular environment, Au(III) complexes are expected to produce Au(I) and metallic gold.

Due to the widespread application of gold species, it is highly desirable to develop suitable detection methods especially those that are applicable in biological systems to monitor the gold mediated physiological processes.

2.1.3. Optical properties

Gold-coordination complexes show biological activities as well as unique optical properties. The nature of the coordinating ligands dictates the luminescence properties of d^{10} Au(I) complexes.[27–29] Au(I) species can make monometallic and dimetallic complexes (Fig. 2) with phosphine, indole-phosphine, alkynyl, pyridine, *N*-heterocyclic carbenes (NHCs), pyrazole, etc.[30–32] Some gold complexes show luminescence in solid state as well as in aqueous solution: for example, Au(I)–triphenylphosphine tris(sulfonate) showed emissions at 494 nm and 515 nm in the solid state and in aqueous solution, respectively.[33]

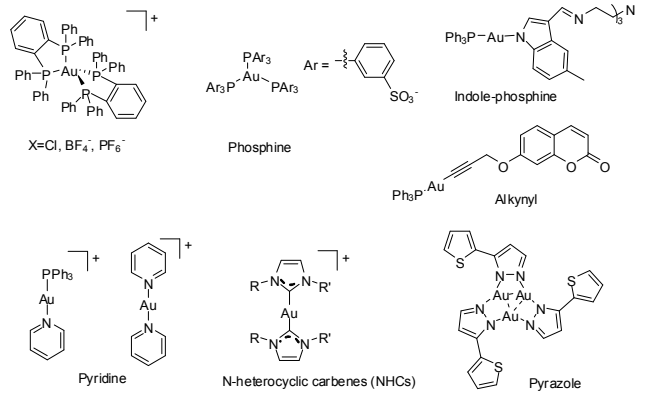

Fig. 2 Some luminescent monometallic and homometallic Au(I) complexes.

The application of luminescence properties of Au(I) complexes for bioimaging purpose is limited, because these complexes do not possess the requisite solution state luminescence that allows bioimaging by confocal fluorescence microscopy (CFM).[34] To overcome this drawback, at present,

the development of Au(I) complexes for bioimaging purpose is pursued by functionalization of Au(I) with fluorescent ligands, typically known organic fluorophores.[35,36] Ott and Pope investigated series of linear Au(I) complexes incorporated with an ancillary phosphine, alkynyl, thiolated fluorophore, or anthraquinone (Fig. 3).[37–39] These Au(I) species coupled with known organic fluorophores have been investigated for bioimaging applications as well as for potential abilities as drug candidates.[40]

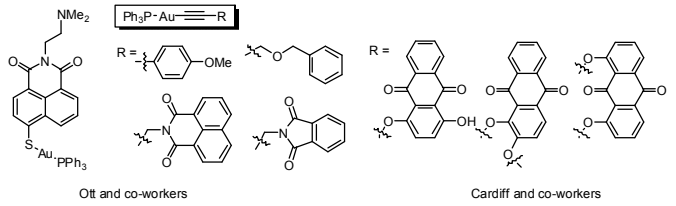

Fig. 3 Au(I)-fluorophore complexes for bioimaging application.

2.1.4. Conventional detection methods

The conventional analytical methods for the detection of gold species mostly rely on the various instrumental techniques such as flame atomic absorption spectrometry (FAAS), graphite furnace atomic absorption spectrometry (GFAAS),[41–43] inductively coupled plasma atomic emission spectrometry (ICP-AES),[44] inductively coupled plasma mass spectrometry (ICP-MS),[45,46] and electrochemical assay.[47] However, these traditional methods require complicated sample preparation and separation procedures prior to analysis, in addition to use of expensive instrumentation with well-trained operators.[48] Some of the methods need chromatographic instrumentation, which has poor quantitative reproducibility especially for the determination of trace amount of gold ions.

In this point of view, the fluorescence spectroscopy with an appropriate sensing molecule, a fluorescence probe or a chemosensor, would provide a highly desirable detection method for gold species. The fluorescence method is widely used for sensing metal species because of its high sensitivity and facile operation.[49,50] Importantly, fluorescence sensing systems that allow *in vivo* and *in vitro* cellular imaging provide reliable tools for studying biological processes involving the target analytes as well as for clinical diagnosis and monitoring of diseases.

Here, we have overviewed recent studies aimed at the fluorescence sensing of gold ions or gold nanoparticles in some cases, by small molecule probes or chemosensors. We have avoided to use "sensor" to indicate the fluorescence sensing systems, as the terminology is used by analytical chemists only for those sensing systems that are capable of continuous monitoring of analytes.

2.2 Fluorescence sensing systems for gold species

Known fluorescent probes for gold ions can be classified into two categories according to the sensing mechanism: (1) the reaction-based and (2) coordination-based probes. The reaction based probes can be further divided into two, depending on whether the sensing reaction involves activation of the alkyne bond or not. According to the classifications, we overviewed the known fluorescent probes by grouping them into three categories.

2.2.1. Fluorescence sensing of gold species through activation of the alkyne bond

Catalytically active gold complexes have common oxidation states of +1 and +3. Typical sources of gold complexes such as AuCl and $AuCl_3$ have strong alkynophilicity, activating the alkyne bond toward oxygen, nitrogen, and even carbon-based nucleophiles. This reaction characteristic inspired several groups to develop the first reaction-based fluorescence sensing systems for gold species. In the late 2009 and early 2010, Yoon and Kim, Ahn, and Tae groups concurrently disclosed rhodamine-based alkyne systems as the reaction-based fluorescence sensing systems for gold species, respectively (Fig. 4). Previously, a related ring-opening followed by cyclization reaction was used for the development of fluorogenic and chromogenic sensing systems for Hg(II), Pb(II) and Ag(I) ions by Tae, Yoon, and Ahn groups, respectively.[51–54] Coordination of $AuCl_3$ or AuCl to the alkyne bond triggered a series of bond reorganizations, involving the rhodamine-spirolactam ring-opening and intramolecular cyclization reactions to yield the heterocyclic ring (Fig. 4). The ring-opening reactions accompanied by turn-on fluorescence and colorless-to-pink color changes, enabling the first fluorescence detection of the gold species with no appreciable interference from potentially competing metal species including Mg(II), Ba(II), Al(III), Cr(II), Mn(II), Fe(II), Fe(III), Co(II), Ni(II), Pd(II), Pt(II), Cu(II), Ag(I), Zn(II), Cd(II), Hg(II), and Pb(II).

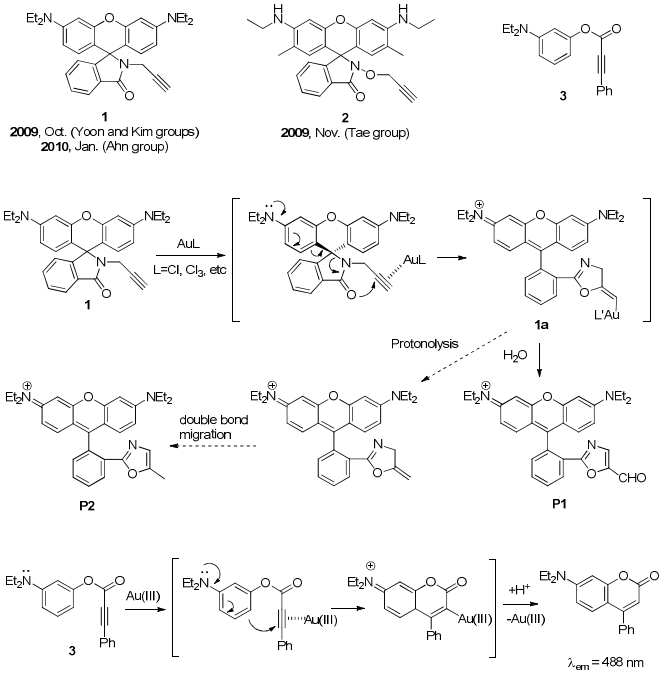

Fig. 4 Fluorescence sensing systems of gold species, probes **1–3**, which are based on the alkyne activation, and sensing mechanisms for probes **1** and **3**, respectively.

The excellent selectivity of the probes indicated that the alkyne activation by gold species is a highly promising sensing strategy. Indeed, this sensing strategy was adopted by others in a number of papers followed.

The rhodamine B derivative **1** (Fig. 4) was independently evaluated in EtOH/HEPES buffer (1:1, v/v, pH = 7.4)[55] or in CH_3CN/PBS buffer (1:1, v/v, pH = 7.2),[56] showing similar sensing properties except the different sensitivity in the case AuCl. This latter discrepancy seemed to be caused by different experimental conditions where AuCl might disproportionate into Au(III) and Au(s) species [3Au(I)(aq) → Au(III)(aq) + 2Au(s)].[57] $AuCl_3$ is hygroscopic and hence should be handled in a glove box for the quantitative sensing purpose.

Similar sensing properties were obtained by the rhodamine 6G-based probe **2** (Fig. 4) in PBS buffer (pH = 7.4, containing 1% MeOH).[58]

According to the sensing mechanism of probe **1** (Fig. 4), the vinylgold intermediate **1a** underwent an unexpected transformation into the formyloxazole **P1** as the major product, rather than producing the methyloxazole **P2** that was expected to be formed through the usual proto-deauration followed by double bond migration processes.[59] A subsequent mechanistic study was carried out by Ahn and co-workers using *N*-(propargyl)benzamides as model compounds, which led to characterization of the corresponding vinylgold intermediates and their reactivity depending on media. It was found that the vinylgold intermediate generated from *N*-(propargyl)benzamide underwent the proto-deauration process in organic media to produce the corresponding methyloxazole as the major product, whereas, in aqueous media, it took the unusual reaction route to produce the corresponding formyloxazole as the major product.[56]

Kim and co-workers subsequently reported another type of alkyne activation approach to sense gold species,[60] in which a phenyl ring participated in a gold ion-mediated cyclization. The aryl alkynoate **3** (Fig. 4) thus underwent gold ion-promoted hydroarylation to produce a fluorescent coumarin, enabling turn-on sensing of Au(III) ions. A small response from Ag(I) was observed among various typical metal ions screened. The poor sensitivity of the probe toward AuCl reflects its lower Lewis acidity compared with $AuCl_3$ toward the carbon–carbon triple bond. A drawback of the sensing scheme is the slow reaction rate, requiring more than one day for signal saturation with 10 equivalents of $AuCl_3$ in ethanol.

The pioneering works concurrently reported by the several research groups ignited subsequent research efforts toward the development of fluorescence sensing systems for gold species based on chemical transformations.

In late 2010, Peng and co-workers reported *N*-propargyl-naphthalimide **4** (Fig. 5), which selectively sensed Hg(II) or Au(III) ions depending on the reaction media and pH.[61] In HEPES buffer (pH = 7.4, containing 0.05% DMSO), the propargyl group in the probe underwent a regioselective oxymercuration reaction promoted by Hg(II) ions and produced the corresponding keto compound, which process caused the change of the maximum fluorescence emission band of the probe from 543 nm to 486 nm. Under the same conditions, various other metal ions caused slight changes in the emission spectra. In contrast, the probe showed similar ratiometric response only toward Au(III) ions when the reaction medium was changed to MeOH/H_2O (95:5, v/v) and the pH to 9.0. In the test conditions, it required about 5 h for Hg(II) and 12 h for Au(III) ions to yield the product, respectively.

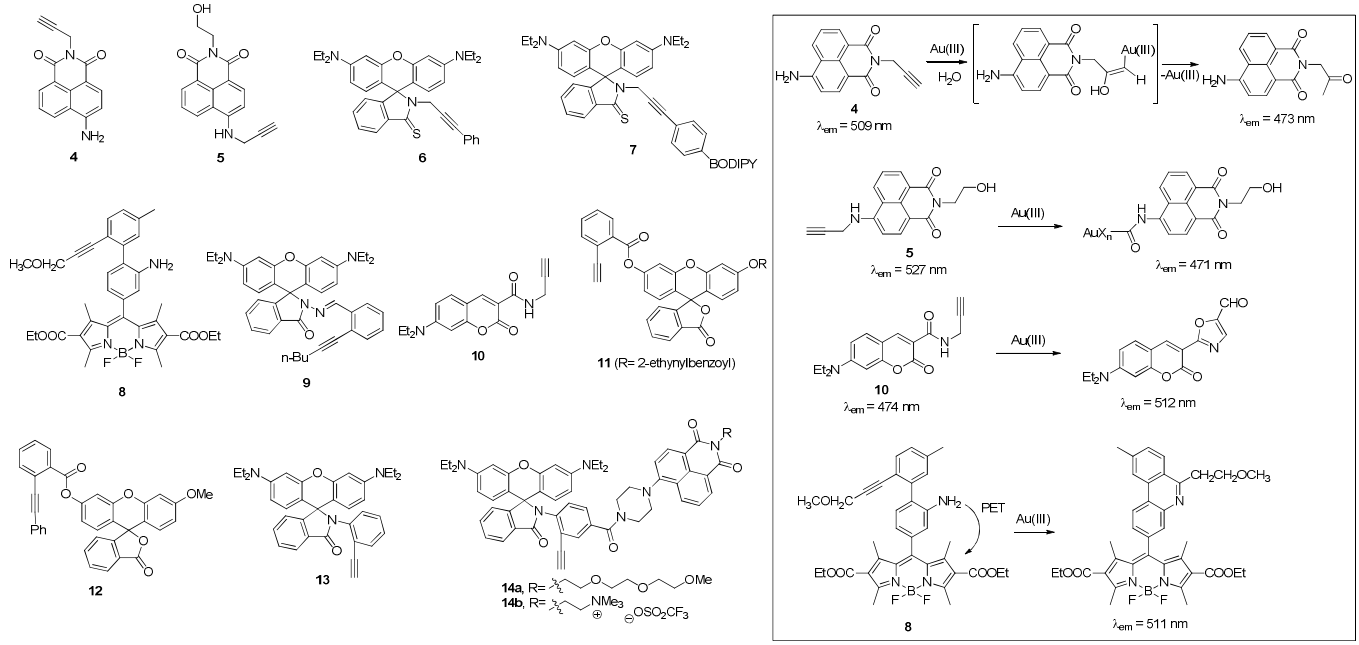

Fig. 5 Fluorescent probes (**4–14**) for gold ions, based on alkyne bond activation and their sensing mechanisms.

Later Yoon and co-workers reported *N*-propargyl-1,8-naphthalimide **5** (Fig. 5), which also responded to Au(III) ions with ratiometric fluorescence change.[62] A Au(III)–acyl adduct was proposed as the sensing product, based on ^{1}H NMR analysis, which conversion induced fluorescence emission shift from 527 nm to 471 nm. Addition of a surfactant, cetyltrimethyl ammonium chloride (CTAC, 50 μM), to a solution of probe (20 μM) in PBS buffer (pH 7.4, containing 4% EtOH) accelerated the sensing reaction from ca. 160 min (buffer alone) to ca. 40 min (in the presence of CTAC) for completion. Under the optimized sensing conditions, the probe showed ratiometric response only toward Au(III) ions and no response toward other metal species. The probe was used for fluorescent imaging of gold ions in HeLa cells.

Lin and co-workers reported a FRET (fluorescence resonance energy transfer) sensing system based on *N*-(3-phenylpropargyl)-rhodamine thiolactam **6** containing a BODIPY dye at the *N*-propargyl site, which sensed Au(III) ions through the alkyne activation strategy. The resulting FRET probe **7** (Fig. 5) selectively sensed Au(III) among various metal species with ratiometric fluorescence change.[63] When probe **7** was titrated with $AuCl_3$ in EtOH/phosphate buffer (7:3, v/v, pH = 7.0), the BODIPY emission band at 514 nm decreased while the rhodamine emission band at 594 nm increased upon excitation at 470 nm. Also, the FRET probe was used for determination of an unspecified amount of gold nanoparticles (AuNPs) in a commercial sample. For the quantification, AuNPs were pretreated with aqua regia to produce gold ions, and then the resulting solution was extensively diluted before sensing with the probe.

Song and co-workers reported a new type of alkyne activation approach to sense gold ions, which involved an intramolecular hydroamination reaction. A BODIPY dye containing a 2'-ethynylbiphenyl-2-amine analogue, probe **8** (Fig. 5), thus underwent Au(III)-mediated cyclization in EtOH/PBS buffer (1:1, v/v, pH = 7.4) to signal turn-on fluorescence change.[64] The conversion rate was a little faster compared to that observed by the propargylamine-derived rhodamine, but requiring still more than an hour for signal saturation. Both Hg(II) and Pd(II) ions interfered the sensing reaction, which caused a substantial reduction in the fluorescence intensity in competition experiments. The probe was used for fluorescent imaging of gold ions HeLa cells.

Emrullahoğlu and co-workers reported a rhodamine-derived sensing system for gold ions, probe **9** (Fig. 5), which underwent the spirolactam ring-opening triggered by a gold ion-promoted alkyne activation to give turn-on fluorescence response.[65] The conversion was effected only by Au(III) ions among various other metal species examined in CH_3CN/HEPES buffer (1:1, v/v, pH = 7.0). The probe was used for fluorescent imaging of Au(III) ions in HCT-116 cells.

Chen and co-workers reported *N*-propargyl-coumarin amide **10** that selectively sensed Au(III) ions with ratiometric fluorescence change (Fig. 5).[66] The formation of 5-formyloxazole ring from the *N*-propargyl amide in the presence of Au(III) ions, an established cyclization reaction in aqueous media, caused emission shift from 474 nm to 512 nm owing to change in the intramolecular charge transfer (ICT).[67] Again, this alkyne activation approach also showed little response from other metal species examined.

Although the aforementioned alkyne activation approaches have been demonstrated to be a powerful strategy to develop fluorescent probes for gold ions, in particular, with very high selectivity, potential drawbacks such as the high percentage of an organic co-solvent used, slow reaction rate, or interference from side reactions remained to be addressed. For example, the gold sensing process with probe **1** could also produce two types of nonfluorescent compounds in approximately 30–40% yields of the total mass. Simple hydration of the acetylenic moiety promoted by Lewis acidic gold species could compete with the spirolactam ring-opening process. Furthermore, an unusual ring-closing process was found to compete with the sensing process, producing a tricyclic vinylgold(III) species that was nonfluorescent.[68] The formation of such nonfluorescent side products would be dependent on the sensing conditions such as the reaction medium,[69] temperature, concentration, etc, which would undermine the reliability of the quantification data. Also, the formation of nonfluorescent side products would lead to lowering of the detection limit.

Ahn and co-workers disclosed a new sensing scheme for gold species, in which the reaction site was separated from the signaling unit to alleviate the side reactions observed in the rhodamine-based probe **1**. A fluorescein bis-(2-ethynyl)-benzoate, probe **11** (R = 2-ethynylbenzoyl) thus prepared (Fig. 5), underwent Au(III)-promoted ester hydrolysis, which accompanied turn-on fluorescence change in HEPES buffer (pH = 7.4, containing 0.25% DMSO).[68] Other possible side reactions including the simple hydration of the ethynyl moiety were found to be negligible. The conversion was quite fast and completed within 1 h at ambient temperature. The sensing scheme was also highly selective to Au(III) among various metal ions examined, except Hg(II) that showed a minor interference.

A similar sensing scheme was concurrently disclosed by Patil and co-workers. A fluorescein mono-(2-phenylethynyl)-benzoate, probe **12** (R = 2-(phenylethynyl)benzoyl), thus sensed Au(I) ions in CH_3CN/PBS buffer (1:1, v/v, pH = 7.4) with turn-on fluorescence change (Fig. 5).[70] Other metal species showed negligible interference. Fluorescence images of A549 cells pre-incubated with AuCl were obtained using the probe, but with limited resolution because of the poor emission behaviour of the hydrolyzed product, fluorescein mono-methyl ether, as noted by Ahn and co-workers.[68]

The aforementioned ester-type probes such as **11** and **12** pose limitations in bioimaging owing to the ubiquitous esterase activity in living systems.[71] Recently, Ahn and co-workers disclosed a novel approach to suppress the side reactions in gold-sensing systems based on alkyne activation as well as to avoid the esterase activity observed in the ester-type probes. To enhance reactivity of the original probe **1** and, hence, to suppress the side reactions observed, they raised steric strain around the rhodamine lactam moiety by substituting the *N*-

propargyl group in the original probe **1** with *N*-(2-ethynylphenyl). As-prepared probe **13** (Fig. 5) thus underwent the Au(III)-mediated ring-opening reaction faster than the case of probe **1**, with about 4.5 times larger pseudo-first-order rate constant [k_{obs} = 0.13 min^{-1} for **13**, k_{obs} = 0.029 min^{-1} for **1**; measured in CH_3CN/PBS buffer (1:1, v/v, pH = 7.0) at 25 °C], which was ascribed to the ground-state elevation.[72] The rate acceleration in turn suppressed the competing alkyne hydration that was a non-signaling process, in addition to the hydroarylation side reaction observed in the probe **1**. As a result, the probe showed very high sensitivity, enabling detection of Au(III) ions down to 0.5 ppb level. Furthermore, a FRET sensing system (**14a** and **14b**) was constructed by introducing a naphthalimide dye to the *N*-phenyl ring of the probe **13** (Fig. 5).

Interestingly, the FRET system showed even faster response to gold ions than its parent compound **13**; the fluorescence change was almost complete within 20 min when the probe at 10 μM was treated with an equivalent amount of $AuCl_3$ in CH_3CN/PBS buffer (1:9, v/v, pH = 7.4) at 25 °C. It should be noted that most of the known probes based on alkyne activation show rather slow response toward gold ions. Under the titration conditions, an emission band of the naphthalimide at 520 nm diminished while that of the rhodamine at 587 nm increased, showing ratiometric response.

Table 1 Sensing characteristics of probes **1-14**.

Compd.	Selectivity	Sensitivity, LOD;[a] response time	Bioimaging data	Others	Ref
1 (Yoon)	Au(III)	▪ 63 ppb in EtOH/H_2O (1:1, v/v) ▪ Saturation: 30 min. (10 eq.)	▪ Imaging of HaCaT cells [Au(III)]	▪ DMSO or EtOH/HEPES buffer (1:1, v/v, pH = 7.4) ▪ Chemodosimeter (LOD: 100 ppb in EtOH/HEPES buffer system) ▪ NMR and Mass analysis for the product	55
1 (Ahn)	Au(I), Au(III)	▪ 0.4 ppm ▪ Saturation: 20 min. (3 eq.)	▪ Not reported	▪ CH_3CN/PBS buffer (1:1, v/v, pH = 7.2) ▪ NMR and Mass analysis for product ▪ Reaction mechanism studied	56
2	Au(III)	▪ 50 nM ▪ Saturation: 80 min. (2 eq.)	▪ Imaging of HeLa cells [Au(III)]	▪ Rhodamine 6G fluorophore ▪ PBS buffer (containing 1% MeOH), pH = 7.4 ▪ NMR analysis for the product	58
3	Au(III)	▪ 64 ppb ▪ Saturation: >16 h (10 eq.)	▪ Imaging of HaCaT cells [Au(III)]	▪ In EtOH ▪ Au(III)-catalyzed hydroarylation reaction ▪ Slow reaction	60
4	Au(III)	▪ Not reported ▪ Saturation: 20 min. (36 eq.)	▪ Not reported	▪ MeOH/H_2O (95:5, v/v, pH = 9.0) ▪ Ratiometric ▪ NMR and Mass analysis for the product	61
5	Au(III)	▪ 8.44 μM ▪ Saturation: 60 min. (5 eq.)	▪ Imaging of HeLa cells [Au(III)]	▪ PBS buffer (containing 4% EtOH), pH = 7.4 ▪ Surfactant (CTAC) for the enhanced rate ▪ Ratiometric	62
6	Au(III)	▪ Not reported ▪ Saturation: Not reported	▪ Not reported	▪ EtOH/PBS buffer (7:3, v/v, pH = 7.0) ▪ Turn-on type ▪ No Hg(II)-mediated ring-opening	63
7	Au(III)	▪ LOD: 37 μM ▪ Saturation: 15 min. (3 eq.)	▪ Not reported	▪ EtOH/PBS buffer (7:3, v/v, pH = 7.0) ▪ FRET system ▪ Quantitative detection of AuNPs	63
8	Au(I), Au(III)	▪ 63 ppb ▪ Saturation: 60 min. (5 eq.)	▪ Imaging of HeLa cells [Au(III)]	▪ EtOH/PBS buffer (1:1, v/v, pH = 7.4) ▪ Turn-on type (PET process) ▪ Au(III)-catalyzed intramolecular hydroamination	64
9	Au(III)	▪ 0.6 ppm ▪ Saturation: 60 min. (5 eq.)	▪ Imaging of HCT-116 cells [Au(III)]	▪ CH_3CN/HEPES buffer (1:1, v/v, pH = 7.0) ▪ Monitoring gold ions in synthetic samples ▪ NMR and Mass analysis for the product	65
10	Au(III)	▪ 44 μM ▪ Saturation: 20 min. (5 eq.)	▪ Not reported	▪ DMF/HEPES buffer (6:4, v/v, pH = 7.4) ▪ Ratiometric ▪ Mass analysis for the product	66
11	Au(III)	▪ 0.4 μM ▪ Saturation: 60 min. (2 eq.)	▪ Imaging of HeLa cells (fail to get imaging)	▪ HEPES buffer (containing 0.25% DMSO), pH 7.4 ▪ Sensing properties: R_1 = H, R_2 = 2-ethynylbenzoyl ▪ Limits for bioimaging due to esterase hydrolysis	68
12	Au(I)	▪ Not reported ▪ Saturation: 30 min. (10 eq.)	▪ Imaging of A549 cells [Au(III)]	▪ Sensing properties: R_1 = Ph, R_2 = Me derivatives ▪ CH_3CN/PBS buffer (1:1, v/v, pH = 7.4) ▪ Esterase resistance: Porcine liver esterase	70
13	Au(I), Au(III)	▪ 0.5 ppb ▪ Saturation: 60 min. (1 eq.)	▪ Not reported	▪ CH_3CN/HEPES buffer (3:7, v/v, pH = 6.0) ▪ Oxazine product formation (no side product) ▪ DFT calculation	72
14	Au(I), Au(III)	▪ Not reported ▪ Saturation: 20 min. (1 eq.)	▪ Imaging of N2A cells (**14a**: low permeability) (**14b**: good permeability)	▪ CH_3CN/PBS buffer (1:9, v/v, pH = 7.4) ▪ FRET system ▪ Low cytotoxicity	72

[a] LOD: limit of detection.

The probe also sensed $(CH_3CN)Au[P(t\text{-}Bu)_2(2\text{-biphenyl})]SbF_6$, a stabilized gold(I) species, with a linear ratiometric change depending on the concentration of gold ions. One of the FRET probes, probe **14b**, was used to obtain fluorescence images of the probe itself (green emission) and Au(III) ions (red emission) in N2A cells that were pre-incubated with $AuCl_3$.

In this section, we overviewed fluorescent probes for gold ions based on the alkyne activation approach. Other sensing characteristics are summarized in Table 1.

2.2.2. Other types of reaction-based sensing systems for gold species

In 2011, Lin and co-workers disclosed that a condensation product between rhodamine 6G hydrazide and phenyl isocyanate, the compound **15** (Fig. 6), underwent fast hydrolysis to the parent rhodamine promoted by Au(III) ions, which resulted in turn-on fluorescence change.[73] This conversion is interesting considering that a related condensation product with phenyl isothiocyanate forms a heterocyclic ring promoted by Hg(II) ions, making it a turn-on sensing system.[74] The chemical conversion in PBS buffer (pH 7.4, containing 0.3% DMF) proceeded fast only in the presence of Au(III) among various other metal species examined. The probe was used for fluorescent imaging of HeLa cells pre-incubated with $AuCl_3$. The corresponding analogue derived from rhodamine B hydrazide showed slower response.

Later, fluorescent sensing systems based on another type of Au(III)-promoted hydrolysis reaction were also reported. Emrullahoğlu and co-workers reported a dual sensing system for Au(III) and Hg(II) ions, probe **16** (Fig. 6), which is composed of rhodamine B and BODIPY dyes linked together by an hydrazide imine bond.[75] The imine bond in the probe was hydrolyzed by Au(III) ions in CH_3CN/HEPES buffer (1:1, v/v, pH = 7.0) to give two separate dyes, the rhodamine thiohydrazide and formyl-BODIPY, which can be monitored in the pink and green emission channels, respectively. In the case of Hg(II) ions, the imine hydrolysis did not occur, but the rhodamine thiolactam ring was opened and thus could be monitored in the red channel. The hydrolysis proceeded fast only in the presence of Au(III) ions among various other metal species examined. The probe was used for fluorescent imaging of A549 cells pre-incubated with $AuCl_3$.

The same group applied the imine hydrolysis approach to develop a BODIPY-based fluorescence probe for Au(III) ions. The imine bond in probe **17** thus underwent hydrolysis promoted by Au(III) ions in EtOH/phosphate buffer (1:1, v/v, pH = 7.0) to give fluorescence turn-on response (Fig. 6).[76] The conversion proceeded fast only in the presence of Au(III) and Au(I) ions, and other metal species including Hg(II) did not cause any appreciable change. The probe was used for fluorescent imaging of A549 cells pre-incubated with $AuCl_3$.

Other types of chemical conversions were utilized for sensing Au(III) ions. Kim and co-workers disclosed an interesting approach to sense Au(III) ions, which was based on two conversions: (1) generation of AuNPs from $AuCl_3$ in HEPES buffer[77–79] and (2) carbon–iodide (C–I) bond cleavage on the surface of AuNPs.[80,81]

They found that $AuCl_3$ readily underwent reduction to give AuNPs in HEPES buffer (pH = 7.0) at room temperature, but not in other buffer solutions such as Tris, PBS, and deionized water.

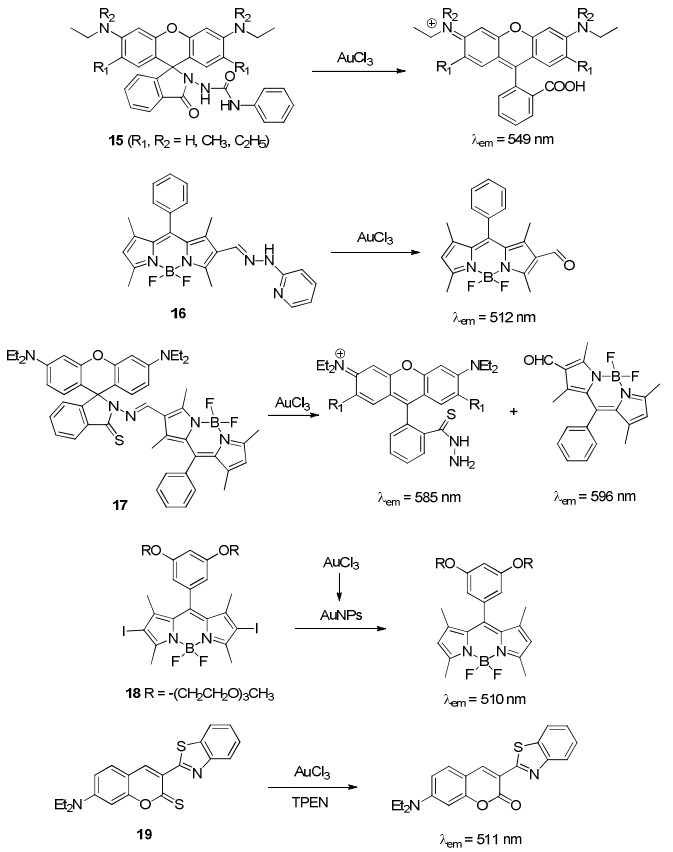

Fig. 6 Other types of reaction-based fluorescent probes (**15–19**) for gold ions and their sensing mechanisms.

They selected an iodo-substituted BODIPY dye, probe **18**, to demonstrate the sensing scheme (Fig. 6).[82] Upon treatment of $AuCl_3$, a EtOH/HEPES buffer (95:5, v/v, pH = 7.0) solution of probe **18**, which is nonfluorescent, emitted green fluorescence (λ_{em} = 510 nm) with linearly increasing intensity depending on the concentration of the gold species. The conversion occurred only by Au(III) and not by other metal species including Au(I). A bromo analogue of the probe showed much slower conversion by $AuCl_3$ under otherwise the same conditions, but caused significant change at higher temperature (65 °C).

Chang and co-workers disclosed a new sensing scheme for Au(III) species, which was based on a desulfurization reaction.[83] A thiocoumarin probe **19** thus underwent Au(III)-promoted desulfurization[84] to give the corresponding keto analogue, which conversion gave turn-on fluorescence change in addition to colour change from pink to yellowish green (Fig. 6). Since the conversion was invented to sense Hg(II) ions originally by Czarnik and co-workers,[85] *N*,*N*,*N*′,*N*′-tetrakis(2-pyridylmethyl)ethylenediamine (TPEN), a masking agent, was

required to suppress interference from other metal species, in particular, Hg(II). As a result, probe **19** in the presence of TPEN underwent the chemical conversion in CH_3CN/acetate buffer (pH = 7.4) only by Au(III), and other metal species gave no appreciable change.

2.2.3. Coordination-based sensing strategy

Along with the reaction-based approach, the coordination-based sensing approach has also been used for the development of fluorescent probes for metal cations. A few reports on the fluorescent probes for Au(III) species are known at the moment (Fig. 7).

In 2012, Lin and co-workers reported a pseudo-coordination-based sensing system for gold ions, probe **20** (Fig. 7). The probe sensed Au(III) through metal-promoted rhodamine ring-opening process, which could be reversed by addition of an excess amount of cyanide; hence, the probe is not a really "reversible" sensing system.[86] The probe selectively sensed Au(III) among other metal species including Hg(II). The result is interesting because a simple rhodamine hydrazide was invented to sense Hg(II) originally by Czarnik and co-workers, as noted by the authors. The Job plot indicated that the probe formed a 1:1 complex with Au(III) ion. The selectivity data were examined in EtOH/H_2O (3:7, v/v), not in a buffer solution, using 20 equivalents of metal species. The probe was used for fluorescent imaging of HeLa cells pre-incubated with $AuCl_3$. Later, Algi and co-workers reported that 2,5-dithienylpyrrole selectively responded to Au(III) ions in the fluorescence quenching mode, probe **21** (Fig. 7).[87] Among various metal species evaluated, only Au(III) caused gradual quenching of the fluorescence at 440 nm depending on the amount of it. The alkynophilicity of gold ion is used in the development of a coordination-based fluorescent probe. In 2014, Rashatasakhon and co-workers disclosed that a 1,8-naphthalimide dye connected with ferrocene through an acetylene bridge, probe **22** (Fig. 7), selectively responded to Au(III) among various other metal species in the fluorescence turn-on mode.[88] The sensing characteristics of other types of reaction-based and coordination-based sensing systems are summarized in Table 2.

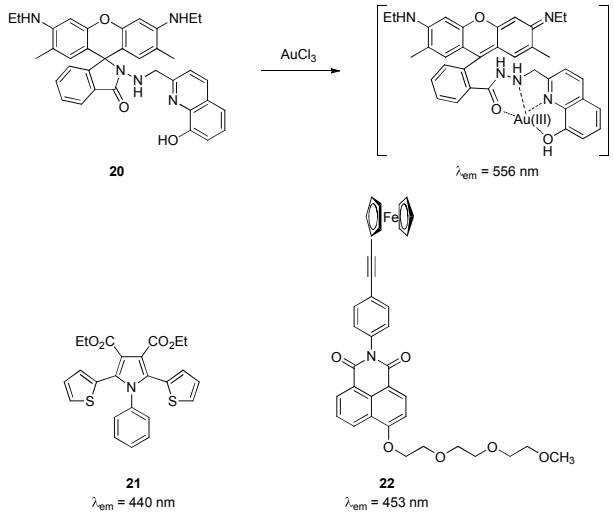

Fig. 7 Coordination-based fluorescent probes (**20**–**22**) for gold ions.

Table 2 Sensing characteristic information of probe **15**-**22**.

Compd.	Selectivity	LOD[a] and response time	Bioimaging data	Other conditions	Ref
15	Au(I), Au(III)	▪ 74 nM ▪ Saturation: 1 min. (10 eq.)	▪ Imaging of HeLa cells incubated with Au(III)	▪ PBS buffer (containing 0.3% DMF), pH = 7.4 ▪ Hydrolysis of acylsemicarbazide to carboxylic acid ▪ Monitoring gold ions in synthetic samples	73
16	Au(III)	▪ 44 nM ▪ Saturation: 30 min. (20 eq.)	▪ Imaging of A549 cells incubated with Au(III)	▪ EtOH/PBS buffer (1:1, v/v, pH = 7.0) ▪ C=N bond hydrolysis reaction ▪ Au-ion binding ligand moiety study	75
17	Au(III)	▪ 65 nM ▪ Saturation: <1 min. (2 eq.)	▪ Imaging of A549 cells incubated with Au(III)	▪ CH_3CN/HEPES buffer (1:1, v/v, pH = 7.0) ▪ Differential detection of Hg(II) and Au^{3+} ▪ Au(III)-catalyzed hydrolysis of the C=N moiety	76
18	AuNPs [from Au(III)]	▪ 0.19 nM ▪ Saturation: 60 min. (>500 eq.)	▪ Not reported	▪ EtOH/HEPES buffer (5:95, v/v, pH = 7.0) ▪ *In situ* AuNPs generation and C-I bond cleavage on the surface	82
19	Au(III) (TPEN)	▪ 11 μM ▪ Saturation: 1 min. (20 eq.)	▪ Not reported	▪ CH_3CN/acetate buffer (1:1, v/v, pH = 4.7) ▪ TPEN: Hg(II) masking agent ▪ Au(III)-catalyzed desulfurization of thiocarbonyl	83
20	Au(III)	▪ 48 nM ▪ Saturation: Not reported (20 eq.)	▪ Imaging of HeLa cells incubated with Au(III)	▪ EtOH/H_2O (3:7, v/v) ▪ 1:1 complex (reversed with excess cyanide) ▪ NMR and Mass analysis for product	86
21	Au(III)	▪ Not reported ▪ Saturation: not reported (8 eq.)	▪ Not reported	▪ Phosphate buffer (containing 0.15% CH_3CN), pH = 7.2) ▪ Coordination-based ▪ Fluorescence turn-off mode	87
22	Au(I), Au(III)	▪ 95 ppb ▪ Saturation: 10 min. (100 eq.)	▪ Not reported	▪ CH_3CN/PBS buffer (1:1, v/v, pH = 8.0) ▪ Coordination to carbon–carbon triple bond	88

[a] LOD: limit of detection

2.3. Summary and perspectives of gold detection

Since the reaction-based approach to fluorescently detect gold species was proven to be effective by several groups concurrently, various types of reaction-based fluorescence probes have been developed as overviewed above. As a result, now we can readily quantify gold species in homogenous samples below the ppb level, simply by fluorimetry, with no appreciable interference from other metal species. Application of such fluorescence probes to bioimaging of gold species in living systems is of importance to investigate their biological effects. Although a number of probes were applied to fluorescence imaging of gold species in cells, use of them to tackle real biological issues is far from realty at the moment. In the case of *in vivo* assay, the typical gold species such as $AuCl_3$ will react with biothiols in cells to form the corresponding Au(I) species that would have much lower Lewis acidity and thus may not activate the existing probes. A highly sensitive probe can even sense a stable gold species such as $(CH_3CN)Au[P(t\text{-}Bu)_2(2\text{-biphenyl})]SbF_6$,[72] but it is not known whether other types of gold species conceivable in living systems could activate the probe or not. Therefore, assessment of fluorescent probes toward other types of gold species, rather than AuCl or $AuCl_3$, is necessary, including studies on the fate of gold species in living systems. Also, a probing system for gold nanoparticles in living systems is of great interest, considering that nowadays gold nanoparticles are widely used for bioimaging, photothermal therapy, drug delivery, and so on.

3. Silver

3.1. Silver species

3.1.1. Chemical properties

Silver (Ag) is a group 11 transition metal in the element periodic table, with the atomic number 47. Being a transition metal, silver shows multiple oxidation states (+1, +2 and +3) in addition to the elemental state, but their chemistry is almost exclusively that of the '+1' state with the electron configuration of $[Kr]4d^{10}$. Due to the completely filled 4d subshell, Ag(I) forms diamagnetic complexes with a variety of coordination geometries including linear, two-coordinate complexes, planar three-coordinate complexes and tetrahedral four-coordinate complexes. Although the soft metal ion character of Ag(I) favored its coordination with the soft donor atom such as sulfur, the coordination complexes of Ag(I) with hard atoms such as nitrogen and oxygen are also observed with heterocyclic ligands (pyridine, bipyridine, phenanthroline) and macrocyclic ligands (crowns, cryptands, porphyrins).[89,90]

Silver has been also used in the organometallic[91] and organocatalysis chemistry.[92–94] Although compared to the other transition metal elements, silver containing compounds are rare in organometallic chemistry. The π-bonded Ag(I)–olefin metal complexes study by Winstein and Lucas in 1938[95] is one of the earliest landmarks in organosilver chemistry.[96] Similarly, Ag(I) also has high tendency to form Ag(I)–arene complexes. Although the Ag(I)–carbene complexes were difficult to isolate due to the low stability,[97] still silver complexes are used extensively as catalysts for the reactions in which carbenes are believed to be the reaction intermediates.[98] Synthesis of a bis(carbene)silver(I) organometallic polymer was also possible using 1,2,4-triazole-3-,5-diylidene as a building block (Fig. 8a).[99]

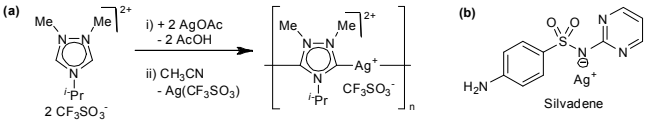

Fig. 8 (a) Synthesis of a bis(carbene)silver(I) organometallic polymer. (b) Structure of an antibacterial drug, silvadene.

Due to the highest electrical and thermal conductivity among the metals, silver has widespread applications and the broad prospects in the electronic industry, and photographic and imaging industry also.

3.1.2. Biological utilities

Silver, along with most of its complexes, is toxic to bacteria, algae, and fungi while it is the least toxic for humans among the elements with such antibacterial effects, called the oligodynamic effect.[100–102] Silver complexes and silver nanomaterials irreversibly bind with the key enzyme systems in the cell membranes of pathogens: they used as antiseptics during the common medical processes to avoid external infections.[103,104] Silver sulfadiazine (silvadene), a silver containing antibacterial drug (Fig. 8b), is well known as a topical cream on burns.

Besides the various applications of silver, much attention has been paid to the negative impact of Ag(I) on the environment, especially on organisms. It is believed that Ag(I) can bind to the amine, imidazole, carboxyl groups of various metabolites such as high molecular weight proteins and metallothionein in tissues of cytosol fractions and enzymes such as sulphydryl enzymes to inactivate.[105–108] Ag(I) can interact with and displace essential metal ions like Ca^{2+} and Zn^{2+} in hydroxyapatite in bone. Repeated silver exposure to human body may cause blood silver (argyria) and urine silver excretion, cardiac enlargement, growth retardation and degenerative changes in the liver.[109] Excessive Ag(I) intake may damage skin and eyes through long-term accumulation of insoluble precipitates.[110]

Although several possible roles of Ag(I) in biological systems have been proposed, such as interaction and inactivation of vital enzymes, binding to DNA, interaction with the cell membrane, and interference with electron transport, still the mechanism of the antimicrobial activity of Ag(I) has not been clarified because of a lack of suitable detection and imaging system.

3.1.3. Conventional detection methods

Similar to the conventional gold detection methods, the detection of silver species also includes various instrumental techniques such as flame atomic absorption spectrometry

(FAAS), graphite furnace atomic absorption spectrometry (GFAAS), inductively coupled plasma atomic emission spectrometry (ICP-AES), inductively coupled plasma mass spectrometry (ICP-MS), and electrochemical assay.[111–115] Other than those instrumental techniques, extraction methods using molecular receptors or chelating ligands are also employed for Ag(I) detection.[116,117]

Compared with the conventional analytical methods, the fluorescence detection methods are highly advantageous as mentioned earlier.[49,50] Also, there is a great demand for imaging the distribution of silver ion in cellular processes with deeper penetration and higher 3D spatial selectivity. In this review, we overviewed the fluorescent and colorimetric silver detection systems with respect to their promising features and sensing schemes.

3.2. Fluorescent and colorimetric detection of silver ions

Based upon the sensing mechanism and platform, the fluorescent and colorimetric detection systems for silver ions are mainly classified into three types: 1) coordination based systems, 2) reaction based systems and 3) others (quantum dots, nanoparticles, polymers and oligonucleotides based).

3.2.1. Coordination-based systems

Due to soft Lewis acid character of Ag(I), it has a high tendency to coordinate with soft Lewis base such as sulfur atoms.[118,119] Hence, silver chemosensors have been developed mainly based on the metal coordination to sulfur containing ligands. Other heteroatoms such as nitrogen and oxygen containing ligands are also used to modulate the binding and signaling in silver ion detection. The coordination based systems are described here under three subgroups, namely: i) coordination to sulfur containing ligands, ii) coordination to non-sulfur containing ligands, and iii) excimer based chemosensors.

3.2.1.1. Coordination to sulfur donor-containing ligands

The sulfur containing ligands used for the development of Ag(I) fluorescence probes are either cyclic or acyclic ligands, which are discussed separately.

3.2.1.1.1.Cyclic ligands

In 1985, Oue and co-workers first reported that benzothiacrown ether **23** (Fig. 9a) had high selectivities for silver ion over other heavy metal ions in cation extraction experiments.[120] They also carried out silver ion spectrofluorimetry by using ion-pair extraction system with thiacrown ether **23** as the cation receptor and eosin Y as the fluorescent anion.[121] Later, introduction of a nitrogen atom in the receptor and direct attachment with a fluorophore led to a fluorescence chemosensor (Fig. 9b). In absence of metal ions, this chemosensor emitted little due to the photo-induced electron transfer (PET)[122] from the amine lone pair to the excited state of the fluorophore. Upon binding of metal ions, the PET process was blocked and fluorescence was turned-on. Based on this sensing strategy, several fluorescence probes for Ag(I) were developed which are described here with their special features.

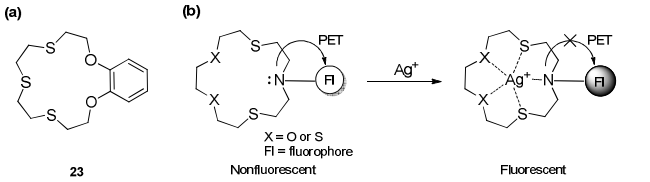

Fig. 9 (a) Structure of a thiacrown ether **23**, and (b) its sensing mechanism of Ag(I).

In 2000, Rurack *et al.* first introduced a thiaazacrown receptor to boron dipyrromethene dye to develop a turn-on type fluorescence Ag(I) probe **24** (Fig. 10).[123] The probe itself emitted weak fluorescence in CH_3CN/H_2O (1:3, v/v). Upon binding of metal ions with the receptor, probe **24** emitted strong fluorescence towards Ag(I) as well as Hg(II) with 1:1 binding stoichiometries for both ions. Later, Lin *et al.* reported compound **25** (Fig. 10) in which the phenyl ring in probe **24** was changed to ortho-methyl substituted one.[124] The detection limit obtained with probe **25** was one order of magnitude lower than the case of **24**. With the addition of 1.1 ppm of Ag(I) (8.42 μM) into the CH_3CN/H_2O (4:1, v/v) solution, drastic enhancement on the fluorescence intensity (>300-fold) of **25** was observed at 509 nm. Other metal ions exerted no influence on the fluorescence intensity of **25** except Hg(II), which showed only less than 2-fold increased intensity at 1.1 ppm (4.5 μM) concentration. But when the ion concentration increased to 4.0 ppm, Hg(II) ion (16.47 μM) also showed a significant fluorescent enhancement by more than 600-fold on the fluorescence intensity of **25**. Although probes **24** and **25** showed high sensitivity towards Ag(I), the interference from the thiophilic metal ion (Hg(II)) remained to be overcome. In the meantime, Schmittel and coworkers also developed iridium(III) and ruthenium(II) complexes **26** and **27** (Fig. 10) with the aza-dithia-dioxa crown-ether receptor for Ag(I).[125] Both compounds **26** and **27** exhibited selective luminescence enhancement toward Ag(I) in CH_3CN/H_2O (1:1, v/v). The emission enhancement factors observed with probes **26** and **27** were 3.4 and 0.3 respectively, indicative of better performance of the former over the latter. All other metal ions showed negligible fluorescence enhancement. However, the addition of Hg(II) quenched the emission of both the probes. Hence, the development of selective fluorescence Ag(I) probe without interference from soft metal ions such as Hg(II) remained as a challenging issue.

For the selective detection of Ag(I) over other soft transition metal ions such as Hg(II), Cd(II), Cu(II) and Tl(I), Shamsipur and co-workers developed a fluorimetric optode membrane based on dansyl dye **28** (Fig. 10).[126] The sensing device detected Ag(I) over a wide concentration range (5.0×10^{-7} to 1.7×10^{-2} M) with fast response (<40 s) in the fluorescence quenching mode.

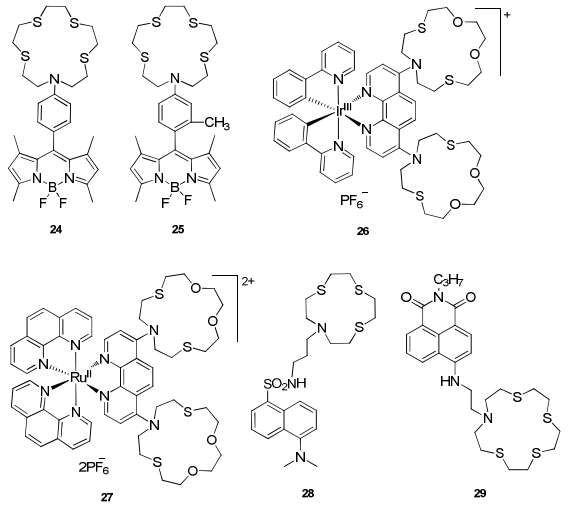

Fig. 10 Structures of fluorescent chemosensors **24–29**.

The fluorescence detection based on such fluorescence quenching rather than enhancement is disadvantageous for a high signal output as well as for bioimaging applications. A naphthalimide dye attached with the tetrathia-aza-crown ether, compound **29** (Fig. 10), showed a similar quenching behaviour toward Ag(I) (Φ = 0.04), owing to an intramolecular d–π interaction between the fluorophore and Ag(I) bound. Weakly fluorescent compound **29** (Φ = 0.06) in EtOH/buffer (1:4, v/v) showed about 5-fold fluorescence enhancement (at 532 nm, Φ = 0.30) upon treatment with Hg(II). When this Hg(II)-bound complex of **29** was treated with Ag(I), its fluorescence was quenched.[127]

The issue of fluorescence quenching due to Ag(I) complexation was later solved by Yoon and Spring group.[128] Usually, chemosensors based on aza-thia-crown ether receptors show high binding selectivity for Ag(I) but signal selectivity for Hg(II), because Ag(I) can quench or silence the fluorescence through enhanced spin-orbital coupling, energy or electron transfer processes. They introduced a carbonyl group between the 1,8-naphthalimide dye and the receptor moiety, leading to a naphthalimide-based probe **30** (Fig. 11). This minor change resulted in fluorescence enhancement of probe **30** in the presence of Ag(I). The conversion of amine to amide functionality resulted in the elevation of the oxidation potential of the fluorophore, and also in sterically blocking of the interaction between the bound Ag(I) and the naphthalimide fluorophore. Significantly, the addition of Ag(I) to the probe induced fluorescence increase by around 14 fold whereas the addition of Hg(II) caused fluorescence increase by 6-fold when measured in CH_3CN/ HEPES buffer (1:1, v/v). Another approach towards Ag(I) selective turn-on type probe **31** was reported by Lee and co-workers. They introduced a different spacer in between the receptor and fluorophore (Fig. 11).[129] The maximum chelation-enhanced fluorescence effect as high as 150-fold (Φ = 0.26) was observed in the presence of Ag(I) with the probe in EtOH/HEPES buffer (1:1, v/v, pH = 7.2).

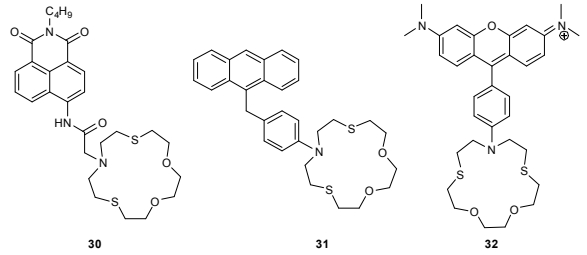

Fig. 11 Structures of chemosensors **30–32** that responded to Ag(I) in the fluorescence enhancement mode.

Although probes **30** and **31** sensed Ag(I) with high sensitivity and a quite good selectivity in the fluorescence turn-on mode, the high content of organic solvent (50%) would limit their use for bioimaging purpose.

Hu *et al.* reported a biocompatible and efficient probe **32** (Fig. 11), which showed enhanced fluorescence towards Ag(I) in HEPES buffer (pH = 7.4).[130] The probe **32** selectively exhibited large fluorescence enhancement towards Ag(I) over Hg(II) or other metal ions with a fast response (<2 min). The selectivity towards Ag(I) over Hg(II) was explained by a difference of the frontier molecular orbital energies calculated. The fluorescence increase at 578 nm showed a linear response to 0.5–5 μM Ag(I) with a detection limit of 1.0×10^{-7} M, which reached the standards of US EPA and World Health Organization (WHO) for drinking water (5.0×10^{-7} M). The probe was also used for imaging of Ag(I) in living cells by fluorescence confocal microscopy: The MCF-7 cells incubated with probe only exhibited almost no fluorescence. By contrast, the cells stained with both the probe and Ag(I) showed an obvious fluorescence in the cytoplasm and nucleolus (organelle inside the nucleus). Lodeiro and co-workers reported that structurally related, aza-trithia-cycles attached to anthracene fluorophore through a methylene linker resulted in fluorescence quenching upon binding an Ag(I) ion, which result inform us that the type of linker as well as the aza-thia-cyclic ligand can govern the sensing property of structurally related probes.[131]

The response behaviours of the turn-on type probes are highly dependent on experimental conditions such as the probe concentration, environmental media, excitation power, etc. Moreover, without response calibration curves in similar conditions, quantification of analyte is difficult. For the quantification purpose, the ratiometric sensing is highly desirable for the easy quantification of Ag(I) by avoiding those experimental effects.[132,133] Accordingly, in 2010, Jiang and co-workers reported the furoquinoline derived Ag(I) probe **33** (Fig. 12), which showed ratiometric behaviour based on the intramolecular charge transfer (ICT) mechanism.[134] The compound, which showed a large Stokes shift (about 173 nm), responded to Ag(I) with a 50 nm red-shift in the emission band and with high affinity (log K = 7.21 ± 0.07 in ethanol). The quantum yield of the probe **33**–Ag(I) complex in ethanol was calculated to be 0.18, which is slightly higher than that of the probe itself (Φ = 0.14). The nitrogen atom in the furoquinoline moiety was involved in the coordination with silver ions,

inducing ICT. The interaction between the silver ion and the nitrogen atom in the furoquinoline moiety enhances the electron-withdrawing ability of furoquinoline that leads to enhanced ICT and thus the red shift observed.

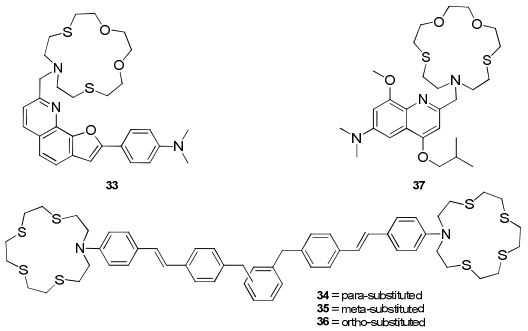

Fig. 12 Structures of the ratiometric fluorescent probes **33–37.**

Recently, another approach towards the ratiometric sensing of Ag(I) was disclosed by Berdnikova and co-workers. The bis(styryl)pyridinium derivatives **34**–**36** (Fig. 12) containing two identical nonconjugated chromoionophores with azadithiacrown ether residues thus gave ratiometric optical response toward Ag(I) and Hg(II) over other metal ions examined.[135] Compounds **34**–**36** showed the emission maxima around 630 nm region in acetonitrile and fluorescence quantum yields in the order of **34**>**35**>**36**. Complex formation with a cation led to hypsochromic shifts of both absorption and emission spectra owing to interaction of the cation with the lone pair electron of the crown ether nitrogen atom in the dye molecule. Nevertheless, the Ag(I) complexes of **34**–**36** emitted much weaker fluorescence than those Hg(II) complexes. Moreover, the ratiometric probes **33**–**36** were examined only in non-biocompatible organic media, such as EtOH or CH_3CN.

A ratiometric Ag(I) probe **37** (Fig. 12) containing the quinolone moiety similar to that of probe **33** was reported by Jiang and co-workers.[136] The probe displayed a weak fluorescence band centered at 565 nm (Φ = 0.05) in MES buffer solution (pH = 6.0). Upon addition of Ag(I), the emission band from the probe gradually decreased with simultaneous arising of a new emission band at 481 nm (Φ = 0.28). A plot of the fluorescence intensity ratio at the two wavelengths (I_{481}/I_{565}) showed a significant increase from 0.19 to 4.99 (up to 26-fold). The resultant complex Ag(I)–**37** displayed a ratiometric and highly selective response to iodide over other anions due to the favorable precipitation of AgI.

3.2.1.1.2. Acyclic ligands

Development of fluorescence Ag(I) probes based on acyclic receptors containing sulfur donor atoms was first reported by Ishikawa *et al.*[137] They studied a series of acyclic podands, open-chain crown compounds, based on sulfur donors that are linked to a fluorophore through nitrogen. It was concluded that the stability of the Ag(I) complexes increased with the number of the sulfur donors in the receptor part of the probe. Among the several acyclic ligands containing compounds, both the compounds **38** and **39** (Fig. 13a) possessed superior binding ability with Ag(I). Accordingly, several fluorescence Ag(I) probes were developed with the general structure feature shown in Fig. 13b.

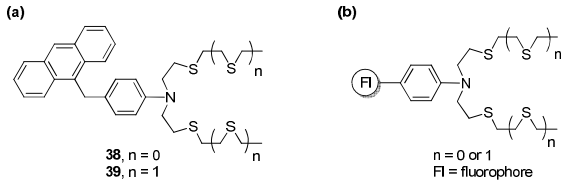

Fig. 13 (a) The structures of the chemosensors **38** and **39**. (b) The general structure of fluorescent Ag(I) probes containing acyclic S-donor ligands.

In 2005, Akkaya and coworkers reported a bis(BODIPY) compound containing the *N*-phenyl-9-aza-3,6,12,15-tetrathiaheptadecane receptor,[138] probe **40** (Fig. 14), which showed ratiometric fluorescence change toward Ag(I) with a large pseudo-Stokes' shift.[139] When excited at 480 nm, the probe dissolved in THF showed very weak residual emission near 550 nm but strong emission centered at 671 nm, as a result of the excitation energy transfer from the left BODIPY dye to the right, π-extended styryl BODIPY dye that emitted in the red region (Fig. 14). The binding of Ag(I) with the podand moiety resulted in a blue shift of the red emission band (41 nm) with an emission intensity ratio (I_{630}/I_{671}) changes from 0.25 to 1.42. Remarkably, the other metal ions including Hg(II) caused only negligible changes in the emission spectrum. The binding constant between the probe and Ag(I) was determined to be as high as 1.7×10^5 M^{-1}. These sensing properties were reported only in THF, a non-biocompatible medium.

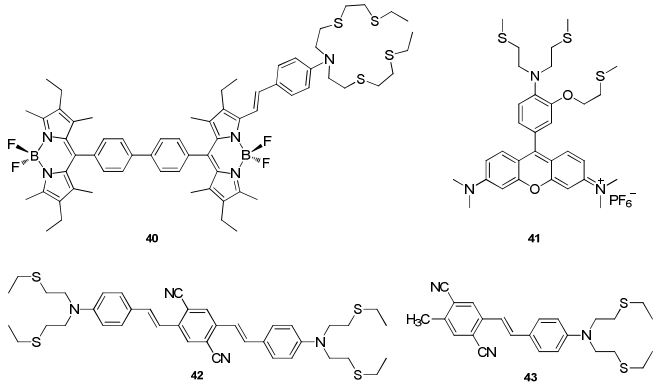

Fig. 14 Structures of fluorescent chemosensors **40–43**.

Fluorescence detection of Ag(I) under physiological conditions (50 mM HEPES buffer, pH = 7.2, and 0.1 M KNO_3) was later reported by Iyoshi *et al.* with a rosamine-based probe **41** (Fig. 14).[140] The probe had a negligible fluorescence quantum yield (Φ<0.005) in the absence of Ag(I) due to the PET quenching process from the aniline nitrogen to of the excited xanthene dye. Upon the addition of Ag(I), however, the fluorescence intensity of **41** increased around 35-fold (Φ = 0.13) at 574 nm. A smaller enhancement in the fluorescence intensity was observed in the presence of Cu(I) and Cu(II). Other

transition metals including Hg(II) had no effect on the fluorescence change. The binding mode of Ag(I) with the chelator moiety of **41** was identified by a crystal structure of the silver complex, which showed a trigonal-planar coordination geometry in which the three sulfur atoms occupied the metal center. The ^{1}H NMR experiments suggested that the aniline nitrogen was associated with the Ag(I) center in the solution, which might inhibit the PET process.

Indolic sulfur–oxygen donor half-crown ethers were also reported to selectively respond to Ag(I) ion but in the fluorescence quenching mode.[141]

Two-photon (TP) probes for Ag(I) were developed based on sulfur containing metal chelates. Two-photon probes can provide higher spatial resolution in bioimaging compared with one-photon probes. Furthermore, the low-energy near-infrared excitation light enables deeper tissue penetration and also alleviates the photobleaching and autofluorescence issues.[142] In 2008, Huang *et al.* reported the first two-photon probe (Fig. 14) for Ag(I), compound **42**.[143] Soon after, they also reported another two-photon probe **43** (Fig. 14) with improved sensing properties.[144] The strong two-photon fluorescence of both the compounds **42** (δ = 1120 GM, TP excitation wavelength = 810 nm) and **43** (δ = 950 GM, TP excitation wavelength = 790 nm) was suppressed upon complexation with Ag(I) in CH_3CN. The suppression in the absorption and emission intensity upon addition of Ag(I) indicated that the large π-electron density of the conjugated systems decreased owing to the binding-induced charge transfer from the aniline nitrogen to Ag(I). Both the compounds showed a notable selectivity to Ag(I) over other potentially competing metal ions. Moreover, probe **43** was successfully used for bioimaging of Ag(I) in live cells. The epithelial cells incubated with the probe in mixed HEPES buffered saline/EtOH/DMSO/CrEL (polyoxyethylene castor oil) (20:35:30:15, v/v/v/v) solution showed uniform and bright orange red fluorescence when fluorescently imaged by two-photon microscopy (TPM). In contrast, the probe treated epithelial cells, after incubation with the HEPES buffer (pH = 7.0) solution containing Ag(I), showed quenched fluorescence. A two-photon probe that shows turn-on or even better ratiometric response to Ag(I) has yet to be discovered, which would provide a powerful tool for imaging of the metal ions in living tissue.

Other than the above mentioned sulfur-containing podands (Fig. 13), a few ligands that contain one sulfur donor atom are known such as thiourea **44**, thiofuran **45**, and thiosemicarbazide **46**, which also showed strong binding affinities with Ag(I) when assisted with non-sulfur hetero atom donors (N or O atoms) at appropriate positions.

Fu and co-workers reported the thiourea **44** that sensed Ag(I) in the fluorescence enhancement mode (Fig. 15).[145] The probe displayed 14-fold enhanced fluorescence (λ_{em} = 385 nm) upon binding with Ag(I) in MeOH/HEPES buffer (3:1, v/v). Job's plot indicated formation of a 1:2 complex between the probe and Ag(I) with an association constant of 1.8 × 10^8 M^{-2}. Among other metal ions examined, interference from Hg(II) (caused 6-fold enhancement) was observed.

Pitchumani and co-workers reported the thiophene **45** that also sensed Ag(I) with fluorescence enhancement (Fig. 15). The probe selectively responded to Ag(I) among various metal ions screened in MeOH/buffer (1:1, v/v, pH = 7.4).[146] The fluorescence enhancement was attributed to an increase in intramolecular charge transfer (ICT) upon binding with Ag(I), supported by a red shift (44 nm) of the probe's emission band that appeared at 359 nm.

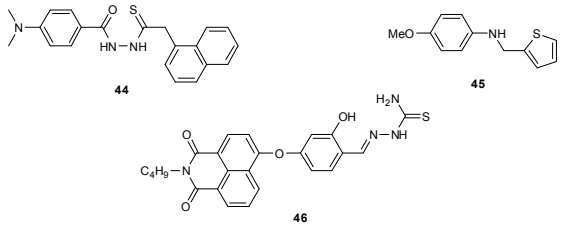

Fig. 15 Structures of the fluorescent chemeosensors **44**–**46**.

The binding of Ag(I) with thiosemicarbazide moiety was also used to develop the naphthalimide based probe **46** (Fig. 15).[147] The probe selectively responded to Ag(I) with 60-fold enhanced fluorescence (λ_{em} = 540 nm) among various metal ions including Hg(II) in EtOH/HEPES (4:1, v/v, pH = 6.5). Two emission peaks at 428 nm and 540 nm were observed, the former of which was ascribed due to the restriction of C=N bond reorganization upon metal chelation. The increase in the fluorescence intensity was attributed to the inhibition of the PET process from the thiosemicarbazide group upon metal binding.

Along with the sulfur-containing functional groups mentioned above, combination of sulfur donor(s) with or without assistance of other heteroatom donor(s) was found to be effective for the selective sensing of Ag(I). Yoon and co-workers reported the thiomorpholine-containing fluorescein **47** that sensed Ag(I) in the fluorescence turn-off mode (Fig. 16).[148] The fluorescence of the probe was quenched upon binding with Ag(I) along with a color change from a light yellow to pink in DMSO/HEPES buffer (5:95, v/v, pH = 7.4). It was proposed that Ag(I) chelates with the sulfur donor and the hydroxyl group of fluorescein.

Anand *et al.* reported a readily accessible disulfide **48** (Fig. 16) containing an anthracene fluorophore, which sensed Ag(I) in the fluorescence turn-on mode with high selectivity over other metal cations in EtOH/HEPES buffer (1:9, v/v, pH = 7.4).[149] Upon addition of Ag(I), the absorption band of probe at 389 nm was red-shifted by 26 nm, resulting in a color change from yellow to colorless. Moreover, the probe emitted weakly (Φ = 0.012) due to the PET blocking and the C=N bond isomerization, but strongly emitted at 440 nm (Φ = 0.24) upon addition of Ag(I). The probe was found to bind with Ag(I) in a 1:1 stoichiometry, with the association constant and the detection limit of 6.407 ×10^2 M^{-1} and 2.797 × 10^{-7} M, respectively. The reversibility of the interaction between the probe and Ag(I) was also confirmed by the addition of Na_2S

into the solution containing the probe and Ag(I), which resulted in weak fluorescence from the dissociated probe.

A supramolecular Ag(I) sensing system was reported by Iki and co-workers.[150] A bimetallic complex between Tb(III) ions and a photon-absorbing thiacalix[4]arene formed a supramolecular coordinate complex with Ag(I), complex **49** (Fig. 16), enabling fluorescence detection of Ag(I) at nanomolar concentrations (3.2×10^{-9} M; 0.35 ppb). The sensing properties of this system were found to be originated from the supramolecular complex formation, and not from the thiacalixarene or Tb(III) individually, demonstrating the first ''supramolecular approach'' to sense Ag(I).

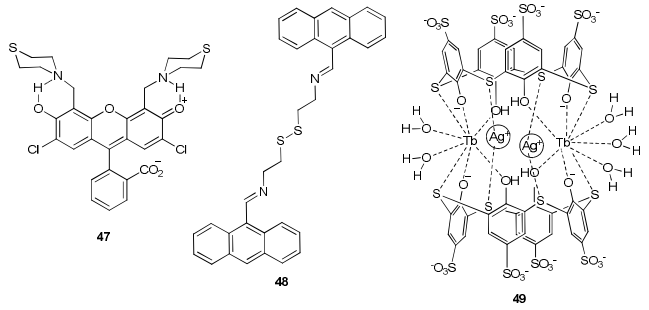

Fig. 16 Structures of the fluorescent probes **47**, **48** and a supramolecular complex **49**.

The aforementioned chemosensors indicate that both the cyclic as well as acyclic S-donor containing ligands are effective for the fluorescence detection of Ag(I). A direct comparison revealed that cyclic ligands generally bind Ag(I) more strongly than the acyclic analogues, plausibly due to the additional stabilization by the macrocyclic effect.[129] But, in general, the chemosensors based on acyclic S-donor ligands show a higher degree of selectivity towards Ag(I), plausibly by reduced binding affinity to the competing metal ions.

3.2.1.2. Coordination to non-sulfur donor containing ligands

Several fluorescence probes for Ag(I) have been developed based on N and O-donor containing ligands. Additional stabilization by Ag(I)–π coordination was also observed for the Ag(I)-complexes in a few cases.

In 2002, Yoon and coworkers reported two pyrazole containing anthracene, **50** and **51**, that sensed Ag(I) in the fluorescence turn-off mode (Fig. 17).[151] The probe **50** responded to both Ag(I) and Cu(II) ions with fluorescence quenching, whereas the probe **51** displayed selective fluorescent quenching only with Ag(I). The 1,8-isomer **50** showed about 100-fold stronger binding affinity toward Ag(I) than the 9,10-isomer **51**, but the former showed only a minor fluorescence change (0.3-fold) whereas the latter showed a larger change (20-fold), upon binding with Ag(I). The larger change observed with **51** was explained by the π-cation interaction involved only in this case.

Several other Ag(I) selective probes that also contain N-donors only (**52** and **53**)[152,153] or contain both N- and O-donors (**54**, **55**, and **56**)[154,155] (Fig. 17) are known; however, all of which showed fluorescence quenching upon binding with Ag(I), either due to the heavy metal effect (for **52** and **54**) or the reduction of ICT in the fluorophores attached (for **53**, **55**, and **56**).

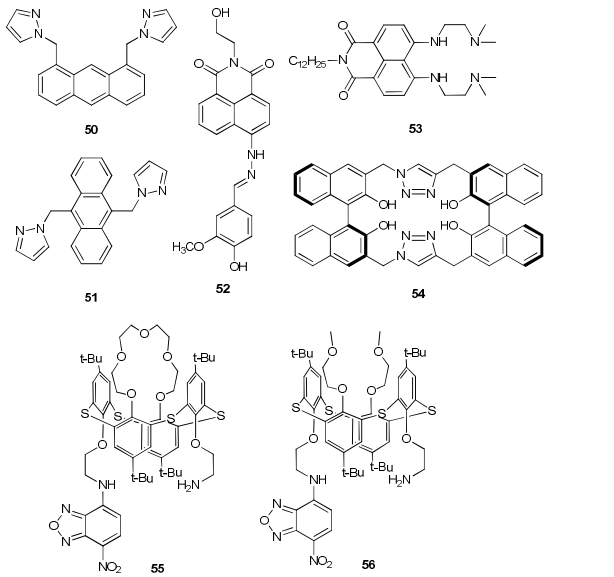

Fig. 17 Structures of chemosensors **50–56** that show Ag(I)-induced fluorescence quenching.

Kim and Yoon groups reported calixarene derivatives **57** and **58** bearing an azacrown ether as Ag(I) binding site and pyrene as signaling part (Fig. 18).[156] The probes contain an additional crown ether, which can bind with other metal ions such as K(I) (**57**) or Cs(I) (**58**). In ethanol, upon the addition of Ag(I), the chelation enhanced fluorescence (CHEF effect) was observed for both **57** and **58** owing to the binding of Ag(I) at the azacrown site with a strong binding constant ($K_a = 6.0 \times 10^3$ M^{-1}). But, after the addition of K(I) to the solution containing **57** and Ag(I) (10 eq.), chelation enhanced fluorescence quenching (CHEQ) was observed due to the complexation of K(I) into the crown ether site which induced the decomplexation of Ag(I) from the azacrown site due to metal-metal ion repulsion. In the case of **58** that contained the crown-6 moiety for binding with Cs(I), the fluorescence from **58**–Ag(I) complex gradually decreased upon addition of cesium ion (0–10 eq.). The results established that the source of the binding selectivity towards Ag(I) comes from the calixarene and azacrown moieties.

Several other fluorescence probes (**59**–**62**) for Ag(I) have been developed based on the PET mechanism of fluorescence signaling (Fig. 18). Among those, the naphthalimide-based probe **59** (Fig. 18) developed by Qian and co-workers is capable of bioimaging.[157]

The probe selectively responded to Ag(I) with turn-on fluorescence change at 533 nm among various other metal ions in EtOH/Tris buffer (4:6, v/v, pH = 7.5). The Job plot indicated formation of a 1:1 complex between the probe and Ag(I), and the association between them was determined to be 9.0 (± 0.5) $\times 10^5$ M^{-1}.

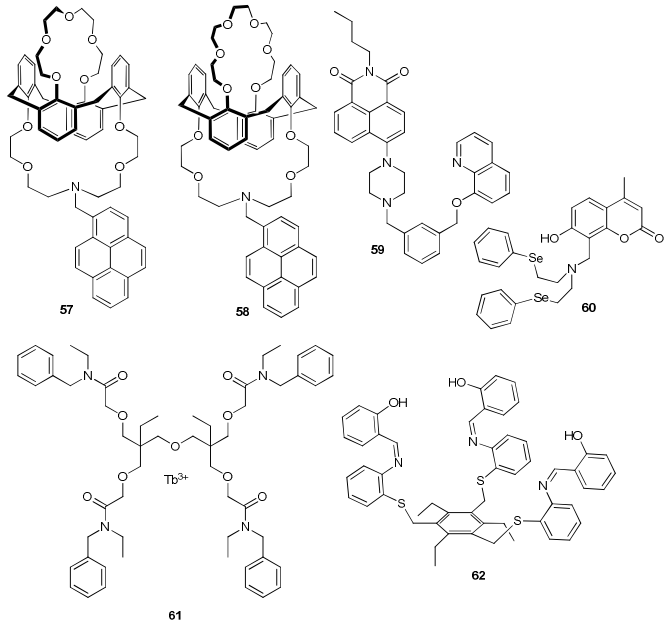

Fig. 18 Structures of fluorescent Ag(I) chemosensors **57–62** that are based on the PET process.

It was proposed that the N- and O-atoms of 8-alkoxyquinoline as well as the N-atoms of pyridine and piperazine moiety are responsible for the metal binding. The probe was used to obtain bright green fluorescence images of Hela cells that were pre-incubated with Ag(I).

Use of high selenophilicity of Ag(I) was explored by Huang *et al*., to develop the fluorescence probe **60** (Fig. 18).[158] The probe sensed Ag(I) with enhanced fluorescence (4-fold), plausibly through inhibition of PET quenching. The probe showed excellent selectivity toward Ag(I) over other competing metal ions, especially Cu(II) and Hg(II) that are common interfering cations in many cases.

Amine associated PET quenching of lanthanide luminescence was also used by Dang *et al.*, to develop fluorescence probe for Ag(I).[159] Thus, the Tb(III) complex of the ligand **61** (Fig. 18) in methanol exhibited partially quenched fluorescence due to the PET process from the "free" nitrogen lone pairs. However, upon addition of Ag(I) the terbium complex showed a noticeable fluorescence due to the binding of the nitrogen atoms with Ag(I). Interestingly, other metal ions such as Na(I), K(I), Ca(II), Ba(II), and Zn(II), etc. resulted no increase in the emission intensity or a faint fluorescence, despite their binding interactions with the nitrogen atoms as suggested by the corresponding absorption spectral changes.

Hundal and co-workers reported the benzene-based tripodal imine **62** (Fig. 18) that sensed Ag(I) with fluorescence enhancement.[160] The probe emitted weakly at 413 nm, plausibly due to PET quenching. Upon addition of Ag(I), however, the fluorescence was restored by 4-fold in CH_3CN/HEPES buffer (8:2, v/v).

Other than the PET mechanism, charge transfer (CT) mechanism was also used to develop fluorescent chemosensors for Ag(I), as exemplified by **63**–**67** (Fig. 19).

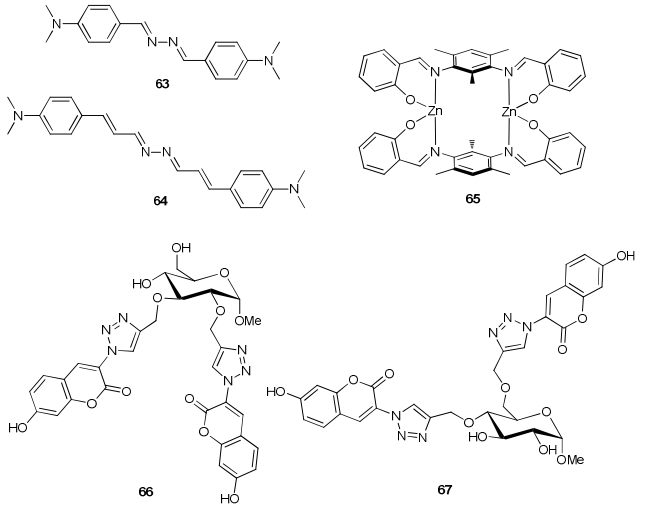

Fig. 19 Structures of the charge transfer based chemosensors **63–67**.

These molecules have two aromatic moieties, which can form CT complexes by intramolecular stacking. Introduction of Ag(I), which can interact with the aromatic rings through cation-π interactions, would disturb the CT complexes and thus induce fluorescence change.

The azine compounds **63** and **64** (Fig. 19) reported by Bharadwaj and co-workers, exhibited weak emission with an absorption band due to intra-ligand charge transfer (ILCT) in the absence of a metal ion in THF.[161] Upon addition of Ag(I) ions, both the azine molecules emited strongly (400-fold) at 487 nm (for **63**) and 560 nm (for **64**) with the binding constant (log β) of 10.32 and 10.54, respectively. Only Cu(I) showed a small enhancement in the emission among other metal ions examined. The emission enhancement is due to the enhanced intramolecular charge transfer (ICT) in presence of the metal ion that withdraws electron density from the donor amine moiety, along with the breaking of the CT complex by metal coordination. X-crystal structures of the Ag(I)-complexes reveal that, in each case, one Ag(I) is bonded to one N-atom of the azine moiety on each side. Each metal ion also showed weak bonding interactions with two C-atoms of the benzene ring.

Later, Pandey and co-workers reported the binuclear zinc(II) complex **65** (Fig. 19) that showed selective "on-off-on" fluorescence switching behaviour in presence of Cu(II) and Ag(I), respectively.[162] The complex emitted strong fluorescence in CH_3CN/Tris buffer (3:7, v/v, pH = 7.0), which was quenched upon addition of Cu(II) but enhanced upon addition of Ag(I). The fluorescence quenching in the presence of Cu(II) was attributed to the metal-to-ligand charge transfer (MLCT), whereas the fluorescence enhancement in the presence of Ag(I) was attributed to the ligand-to-metal charge transfer (LMCT). The weekly emitting Cu(II) complex fluoresced strongly in presence of Ag(I), which observation suggested that Ag(I) could interact with the ligand more strongly than Cu(II); this was further supported by the higher association constant (log K_a = 8.05) observed for Ag(I) than that of Cu(II) (log K_a = 3.29).

The chemosensor **65** was also demonstrated to act as a molecular keypad lock system.

Another example of CT complexes was reported by Shi *et al.,* compounds **66** and **67**, which consisted of two triazolyl coumarin dyes installed onto the glucose (Fig. 19). These compounds exhibited enhanced fluorescence in presence of Ag(I) in an aqueous solution.[163] It was suggested that the two triazolyl coumarins coordinate with one silver ion through both the carbonyl groups of coumarin and one of the triazole nitrogens, causing CHEF. The quantum yields of **66** in water increased from 0.04 to 0.10 upon binding Ag(I). The compound **66** showed high selectivity towards Ag(I) over other metal cations and used for the fluorescence imaging of Ag(I) ions in Hep-G2 cells.

Due to the Lewis acid character of Ag(I), it has a tendency to form Ag(I)–π type interaction with electron rich systems. Hence, Ag(I) selective fluorescence probes have been also developed based on the Ag(I)–π interaction, which could not only enhance the binding affinity but also modulate the signaling process.

The tetra-dansylated diphenyl glycoluril **68** (Fig. 20) selectively sensed Ag(I) with the fluorescence enhancement.[164] An NMR study suggested the close proximity of Ag(I) to the dansyl aromatic moiety, plausibly through a cation π-type interaction. As a result, Ag(I) provided certain rigidity to the dansyl moieties, which would cause decrease in the non-radiative deactivation rate of the probe and thus increase in the fluorescence intensity. Fluorescence response of the probe in presence of other metal ions was almost negligible compared to that of with Ag(I). In 2013, Chao and co-workers reported the gold(I) acetylide complex **69** (Fig. 20) that also selectively sensed Ag(I) through the Ag(I)–π interaction.[165] Upon addition of Ag(I) into a solution of the probe in DMSO, around 18-fold enhancement in the emission intensity at 472 nm was observed under excitation at 311 nm, together with luminescence color change from blue-violet to blue-green.

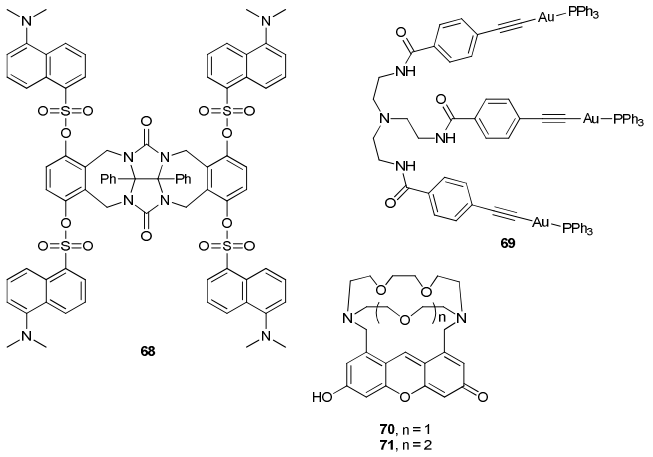

Fig. 20 Structures of fluorescent Ag(I) chemosensors **68**–**71** that are based on the Ag(I)–π interaction.

The σ-bonded Au–acetylide group usually emit from the $^3(\pi\pi^*)$ excited state, which may be perturbed upon binding of Ag(I) at the acetylide group through Ag(I)–π interaction: It was suggested that the flexible nature of the probe would allow for conformational changes upon Ag(I) binding, which would bring the three arms close to each other and thus increase the possibility of forming intramolecular interactions among three Au atoms. The binding stoichiometry and affinity of the probe (log *K*) with Ag(I) were determined to be 1:1 and 4.56 ± 0.21 in DMSO, respectively. The detection limit for Ag(I) was estimated to be 1.0×10^{-6} mol dm^{-3}. The control experiments were also carried to indicate that the acetylide groups and tripodal structures were responsible for the binding of Ag(I).

The Ag(I)–π interaction could also give additional stability during the complexation, as exemplified by the fluorescence probes **70** and **71** that were reported by Ojida and co-workers (Fig. 20)[166] Both the probes showed high selectivity to Ag(I), which was ascribed due to the additional stability by the Ag(I)–arene interaction that was supported by X-ray crystallography and NMR analysis for the Ag(I) complex. A notable feature is that both the probes show ratiometric fluorescence changes toward Ag(I) in MeOH/HEPES buffer (1:1, v/v, pH = 7.4). Upon addition of Ag(I), the emission band of **70** at 524 nm shifted to 554 nm ($\Delta\lambda_{em}$ = 30 nm) with the intensity ratio (I_{554}/I_{524}) change from 0.32 to 11.0. The binding stoichiometry was determined to be 1:1 by the Job plot, the binding constant was $K_a = 4.53 \times 10^5$ M^{-1}, and the detection limit for Ag(I) was 65.6 nM. The probe **71** that has a diaza-18-crown ether also behaved similarly, but with inferior sensing properties ($\Delta\lambda_{em}$ = 10 nm: from 526 nm to 536 nm; I_{536}/I_{526} = 0.77: from 0.74 to 1.51; $K_a = 2.89 \times 10^5$ M^{-1}).

Some dyes show enhanced emission upon aggregation, which phenomenon is called as the aggregation-induced emission enhancement (AIE or AIEE). Thus, AIE fluorophores usually exhibit weak fluorescence in solution, but they become strongly emissive in the aggregate state due to the restriction of the rotational freedom. The AIE phenomenon has been explored in the development of fluorescence probes in recent years. Among the AIE fluorophores, tetraphenylethylene (TPE) has received much attention due to synthetic feasibility and good photophysical properties.

Liu *et al.* reported the adenine-tagged TPE **72** as a Ag(I)-selective AIE probe (Fig. 21).[167] The emission band of the chemosensor at 470 nm increased gradually with increasing amount of Ag(I) in THF/H_2O (1:5, v/v). The fluorescence enhancement was attributed to the selective coordination of the adenine moieties with Ag(I) ions, leading to formation of coordination complexes that formed aggregates due to the low solubility. Later, Ye *et al.* reported another AIE-based chemosensor **73** (Fig. 21) that sensed Ag(I) selectively with a ratiometric fluorescence change.[168] The chemosensor emitted rather weakly (at 435 nm); however, after addition of Ag(I), a new emission band at 485 nm appeared with increasing intensity up to the point where the ratio of [Ag(I)]/[**73**] is below or equal to 2:1. The binding stoichiometry between **73** and Ag(I) was 1:2.

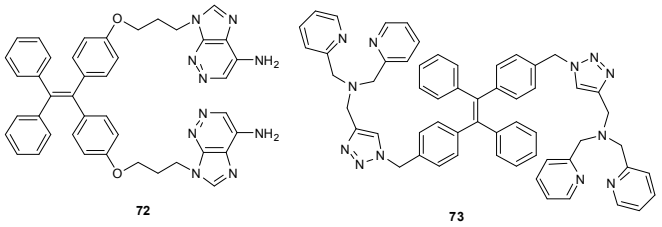

Fig. 21 Structures of the AIE-based fluorescent chemosensors **72** and **73** for Ag(I).

As mentioned above, several strategies have been employed to develop Ag(I) selective fluorescence probes with improved sensing properties. All of the aforementioned probes exhibited absorption and emission bands in the UV–Vis region (200–600 nm) where some biomolecules also absorb light. As a result, autofluorescence from the biomolecules could hamper the signaling process when those probes are used to bioimaging. Moreover, the use of strong energy light (from UV–Vis region) could damage the cells and tissues. Also due to lower penetration ability, tissue imaging is difficult to achieve using the "UV-Vis dyes". To avoid these problems, it is highly desirable to use a fluorophore which can be excited in near-infrared (NIR) region of 650–950 nm.

Wong and co-workers reported the expanded porphyrin[26]hexaphyrin **74** (Fig. 22) that responded to Ag(I) with absorption and emission changes in the NIR wavelength region.[169] In presence of Ag(I), a light reddish color of the expanded porphyrin in MeOH turned to purple and then to blue; correspondingly, the absorption maximum at 543 nm gradually decreased and a new band at 568 nm appeared. In the emission spectra, a sharp decrease in the emission at 1050 nm was observed upon the addition of Ag(I), which was supposed to bind with the pyrrolic nitrogens. Among the other metal ions examined, Cu(II) and Hg(II) also caused a decrease in the NIR emission band.

Zheng *et al.* reported a heptamethine dye containing an adenine group, compound **75**, which selectively sensed Ag(I) with ratiometric fluorescence change (Fig. 22).[170] The compound displayed two emission peaks, at 546 nm and 731 nm, in MeOH/H_2O (1/4, v/v, pH = 5.4 succinic acid–NaOH buffer). When Ag(I) was added to the solution, the emission band at 731 nm decreased while that at 546 nm increased, along with the solution color change from blue to pink. A 2:1 complex between **75** and Ag(I) was observed, which suggested adenine-Ag(I)-adenine binding interaction. The chemosensor exhibited excellent sensitivity towards Ag(I) with a detection limit of 34 nM (ca. 4 ppb). The ratiometric response for Ag(I) was only observed in the acidic pH region (<6.0).

In 2013, Li *et al.* reported another type of heptamethine-based chemosensor, compound **76** (Fig. 22), which sensed Ag(I) at neutral pH.[171] Upon addition of Ag(I) to the chemosensor in EtOH/HEPES buffer (1:40, v/v, pH = 7.0), the absorption band at 764 nm decreased and a new band at 530 nm increased, showing a colour change from blue to light red

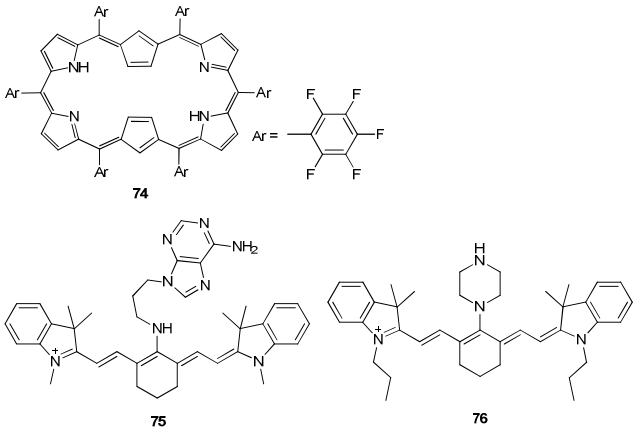

Fig. 22 Structures of the NIR fluorescent chemosensors **74–76**.

Accordingly, the emission band at 758 nm decreased and that at 565 nm increased, with the emission intensity ratio (I_{565}/I_{758}) change from 5.95 to 191 in response to variation of Ag(I) concentration from 0 to 20 μM. Among other metal ions examined, only Ag(I) caused the largest emission change from pH 6.5 to 7.5 with a response time of less than 3 min. The detection limit was determined to be 2.0×10^{-7} M. It was proposed that binding of Ag(I) with the piperazine moiety would shorten the pull-push π-conjugation system of cyanine moiety, causing a large hypsochromic shift in the absorption and emission maxima as observed.

3.2.1.3. Excimer-based chemosensors

A host molecule or fluorescent chemosensor could be structurally fine-tuned to yield a self-assembled sandwich-like dimeric structure in the ground-state, called an excimer, through coordination events by an analyte. In the opposite way, a fluorescent chemosensor that is initially in the excimer state may be converted a monomer upon binding with an analyte. Such excimer-based chemosensors may offer ratiometric changes between the emission intensities from the monomer and excimer.[172] The formation of excimer is highly dependent on the relative proximity between the fluorophores that have flat aromatic moieties. For example, pyrene, a flat and hydrophobic fluorophore, is highly susceptible to form the excimer. As a result, most of the excimer based chemosensors are mainly based on the pyrene fluorophore, except for a few examples of naphthalene. The excimer-based Ag(I) chemosensors thus can be mainly classified according to two sensing modes: i) the monomer-to-excimer conversion, and ii) the excimer-to-monomer conversion.

3.2.1.3.1. Monomer-to-excimer conversion

The excimer-based chemosensors of this type usually exhibit initially a strong monomeric emission from the dye, which upon binding with Ag(I) gradually decreases with concomitant appearance of an excimer emission at the longer wavelength. Accordingly, the ratio of excimer emission intensity to that of monomer emission intensity was used for the ratiometric

sensing of Ag(I). This type of probes thus consists of a fluorophore, mostly pyrene or naphthalene as signaling moiety and a different Ag(I)-specific receptor moiety (Fig. 23).

The first example belongs to this category is the heterocyclic compound **77** (Fig. 23) reported by Yang *et al.*[173] The *N*,*O*-atoms of the heterocycle of **77** were supposed to bind with Ag(I), forming a 2:1 complex between **77** and Ag(I) in EtOH/H_2O (1:1, v/v, pH = 7); the binding event induced the excimer band from the pyrene moieties. A structurally related one, the compound **78** (Fig. 23), was reported by Zhang *et al.*, which also showed the pyrene excimer emission upon binding Ag(I) in methanol.[174] Lee and co-workers also reported a structurally related but water-soluble chemosensor **79** (Fig. 23),[175] which was used to sense Ag(I) as well as silver nanoparticles. Due to the presence of peptide moiety, the chemosensor was able to perform in an aqueous solution containing 1% of DMF or in an aqueous solution at pH 7.4. Upon addition of Ag(I), the monomer emission bands of **79** (at 378 and 395 nm) decreased while the excimer band at 480 nm increased, with the intensity ratio (I_{480}/I_{380}) change from 0.0012 to 0.4358 (ca. 363-fold). Among the other metal ions examined, Hg(II) induced a significant decrease in the monomer emission bands while a small increase in the excimer band. Interestingly, it also showed a ratiometric response to AgNPs, with a ratiometric change in the emission intensities at 500 and 378 nm in aqueous solution. Ratiometric bioimaging of intracellular Ag(I) in HeLa cells was carried out with the probe: blue fluorescence from the probe was changed to green fluorescence in the presence of Ag(I). Before treatment with Ag(I), HeLa cells were washed with a 20 mM HEPES buffer solution (pH = 7.4) containing $NaNO_3$, instead of NaCl, to avoid possible precipitation of Ag(I) ions as AgCl due to the high concentration of cellular chloride ions. A similar approach was reported by Liu *et al.* to sense Ag(I),[176] where the compound **80** (Fig. 23) formed excimer through the coordination between Ag(I) and two adenine (A) moieties at different molecules.

Other than pyrene fluorophore, naphthalene was also used as signaling moiety in a few reports. In 2001, Glass and co-workers demonstrated a cooperative binding-induced excimer formation using two pinwheel systems.[177]

The systems contained four ethylenediamine moieties, which cooperatively interacted with Ag(I) and brought the attached fluorophores in close proximity to induce the excimer emission. Among several fluorophores tested only two fluorophores could induce the excimer band, namely naphthyl-sulfonanilide **81** and pyrenyl acetanilide **82** (Fig. 23).

Later, Zhang *et al.* reported chemodosimeter **83** (Fig. 23) that contained two naphthyl-imidazolium moieties linked to a benzene ring.[178] The high coordinating ability of Ag(I) by the *N*-heterocyclic carbene led to selective sensing of Ag(I) over other heavy transition metal ions examined in CH_3CN/CH_2Cl_2 (1:1, v/v). Coordination of Ag(I) to the benzoimidazolium moieties was suggested to prevent the PET quenching pathway from the excited naphthalene ring to the benzoimidazolium moiety.

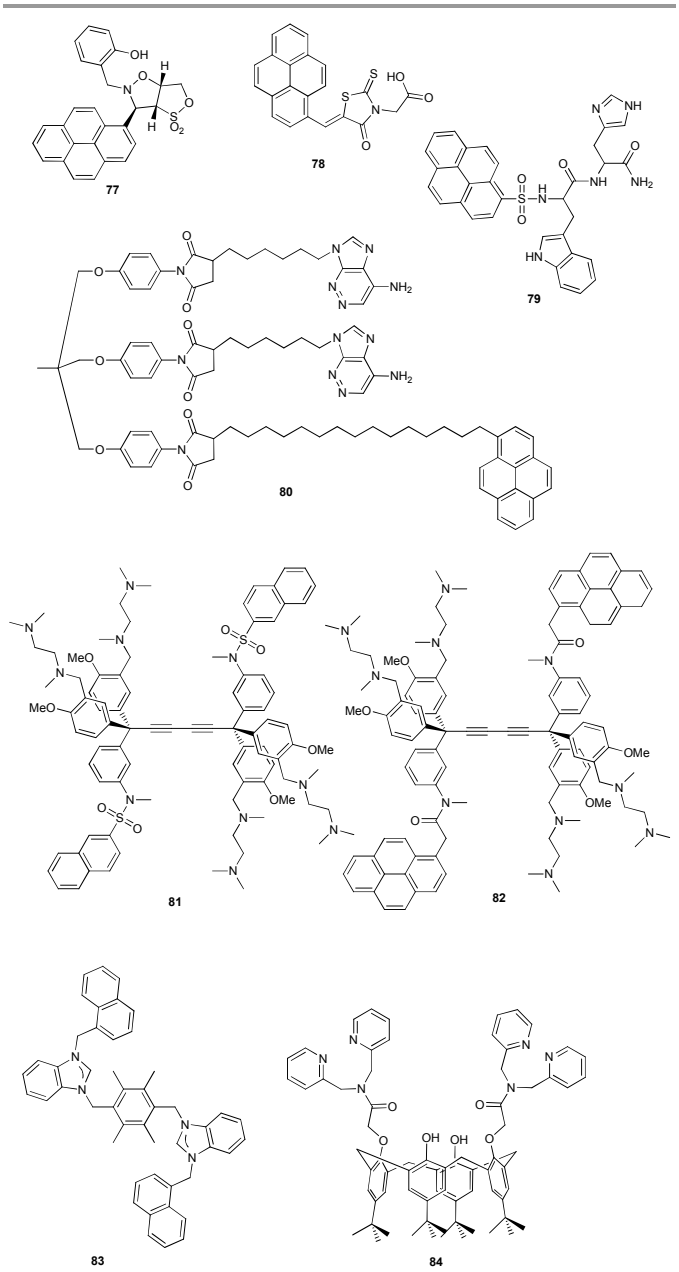

Fig. 23 Structures of fluorescent Ag(I) chemosensors **77–84** based on the monomer-to-excimer formation

Formation of excimer between the pyridyl moieties was also observed with compound **84** (Fig. 23) upon binding with Ag(I), as demonstrated by Rao and co-workers.[179] A tetrahedral complex where Ag(I) bound with the four pyridine nitrogens was established by DFT computations and X-ray crystallographic data.

3.2.1.3.2. Excimer-to-monomer conversion

An opposite mode to the above section is that a chemosensor initially remains in an excimer form due to the strong π–π interaction between the two arene fluorophores, but undergoes conformational change upon binding Ag(I) to form the monomer form. Accordingly, the ratio of monomer emission

intensity to that of excimer emission intensity enables the ratiometric sensing. Several chemosensors of this type containing pyrene fluorophore, **85**–**91**, have been developed through fine tuning of the receptor moieties (Fig. 24).

Liu *et al.* developed a BINOL-pyrene derivative **85** (Fig. 24) by incorporating two pyrene rings through the triazole link that acted as the metal binding site.[180] The chemosensor showed the excimer-to-monomer ratiometric emission change upon binding with Ag(I) in MeOH/H_2O (200:1, v/v). No appreciable spectral change was observed upon addition of other metal ions except Hg(II), which caused fluorescence quenching both for the monomer and excimer emissions. Wang *et al.* reported the bis(pyridylamine) derivative **86** (Fig. 24) that sensed Ag(I) with little inference from Hg(II) as well as other metal ions in DMSO/HEPES buffer (1:1, v/v, pH = 7.4).[181]

Excimer-based chemosensors have been also developed based on the calix[4]arene scaffold, as demonstrated by the chemosensors **87**–**91** (Fig. 24). The thiacalix[4]arene derivative **87** (Fig. 24) reported by Kumar and co-workers, displayed ratiometric response with significant monomer emission enhancement at 377 nm and excimer quenching at 470 nm upon addition of Ag(I).[182] Although the chemosensor possessed high sensitivity towards Ag(I), but it showed strong quenching behaviour towards Fe(III). Concurrently, Yamato and co-workers also reported two Ag(I)-selective fluorescent chemosensors, **88** and **89** (Fig. 24), thiacalix[4]arene derivatives containing two pyrene rings through a triazole link.[183] Both of them, however, suffered from quenching interference from heavy metal ions such as Cu(II) and Hg(II). Later, Chung and co-workers reported another type of calixarene-based chemosensor **90** (Fig. 24), which showed higher metal ion sensitivity compared with the related compound **91** (Fig. 24).[184] Upon the addition of 10 equivalents of Ag(I) in MeOH/$CHCl_3$ (98:2, v/v), the excimer emission of probe **90** (λ_{max} = 476 nm) decreased while the monomer emission (at 379 and 398 nm) increased. This ratiometric response towards Ag(I) was also observed even in 10% aqueous methanol solution. The efficient sensing properties of probe **90** were ascribed due to the specific orientation of the lower-rim triazolylpyrenes, which played an important role for binding with Ag(I). The chemosensor **90** was not only more sensitive among the calix[4]arene-derived excimer-based chemosensors, but also it displayed reduced interferences from the heavy metals (Hg(II), Cu(II)) compared to others.

In general, the excimer based chemosensors which showed monomer-to-excimer formation upon binding of Ag(I) seem to be more efficient with respect to the selectivity over the competing heavy metal ions compared to those chemosensors based on the excimer-to-monomer formation.

3.2.2. Reaction-based sensing systems

The chemosensors described above sense Ag(I) mainly through a reversible coordination with the recognition/receptor part, of which association and dissociation with Ag(I) transduce a fluorescent signal from the fluorophore part.

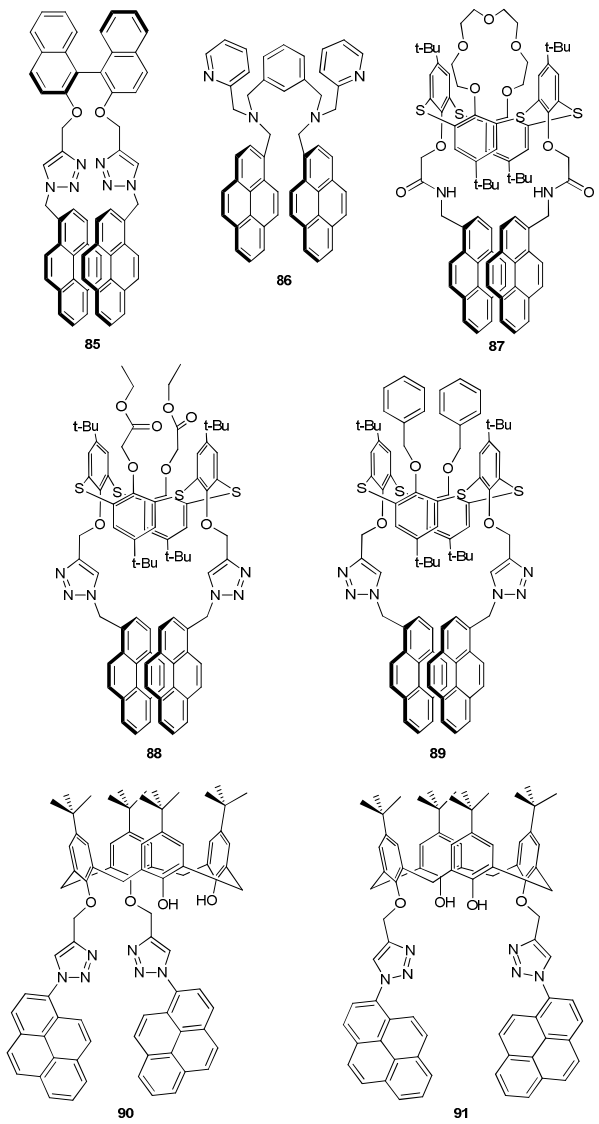

Fig. 24 Structures of fluorescent Ag(I) chemosensors **85–91** based on the monomer-to-excimer formation

In general, such receptor-based chemosensors are desirable for time-dependent monitoring of analytes in biological systems. However, it should be noted that the kinetically inert metal–ligand complexation requires an external, strong ligand to reverse the binding process, which feature would limit use of such metal-coordination based probes for time-dependent monitoring. Another potential limitation of the receptor-based chemosensors is the interference from other metal ions such as Hg(II) that compete with Ag(I) in binding with the receptor moiety. Also, the concentration range governed by the binding equilibrium may limit their practical use. One way to realize very high selectivity and high sensitivity of chemosensors for metal ions is the chemical reaction-based approach, so called the reaction-based or reactive chemosensors, or chemodosimeters. By exploring an analyte-specific chemical conversion to induce fluorescence change, an irreversible but highly selective and sensitive chemosensor can be realized.

Accordingly, many fluorescent chemosensors for metal cations have also been developed; however, it is only recent years that the reaction-based approach to the fluorescent chemosensors for Ag(I) has received much attention from chemists.[49,185]

The colorimetric, not fluorimetric, detection of Ag(I) in aqueous solution was reported by Sun and co-workers, which was based upon the Ag(I) mediated oxidation of 3,3',5,5',-tetramethylbenzidine (TMB) **92** (Fig. 25).[186] When a solution of **92** was treated with Ag(I) at room temperature for 30 min, a colour change from colourless to blue colour was observed with the appearance of three strong absorption peaks centered at 371, 457, and 656 nm, respectively. The colour change was attributed to the oxidation of TMB by Ag(I) to form **92a**. No such colour change was observed in the cases of other metal ions except Fe(III); the interference was solved by using a chelating agent for Fe(III). The detection limit for Ag(I) was estimated to be as low as 50 nM. Later, González-Fuenzalida *et al.* applied **92** for the *in situ* quantification of Ag(I) in the presence of AgNPs.[187] This simple detection method was used to detect the Ag(I) ions adsorbed on the AgNP surface during nanoparticle formation. AgNPs were prepared by three different strategies, one photochemical and two thermal. In all the cases, the yellow solution of AgNPs was turned to blue upon addition of **92**. This colour change indicated the presence of adsorbed Ag(I) ions on the AgNPs surface, which was quantified at a confidence level of 95%.

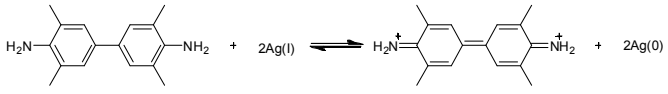

92 92a

Fig. 25 Ag(I)-mediated oxidation of 3,3',5,5',-tetramethylbenzidine (TMB) **92**.

Czarnik and co-workers reported that the anthracene-thioamide **93** sensed Hg(II) as well as Ag(I) with fluorescence enhancement (Fig. 26).[85] This is the first example where Ag(I) is fluorescently sensed through a chemical reaction, here desulfurization. The thioamide group acted as a fluorescence quencher; hence, its conversion to the amide group promoted by Ag(I) ions in water resulted in 55-fold enhancement of the emission band center at 413.5 nm.

Later, the desufurization strategy was adopted by Tsukamoto and co-workers, to develop a coumarin-based system **94** (Fig. 26) that also detected Hg(II) and Ag(I) in the fluorescence turn-on mode.[188] In a phosphate buffer (pH 7.0) containing 0.1% DMSO, the *N*-acetylthioureido compound that was nonfluorescent underwent desulfurization upon treatment with Hg(II) or Ag(I), which conversion resulted in strong fluorescence at 480 nm (400-fold enhancement) within 2 min. The detection limit for Ag(I) was found to be 1 ppb.

The reaction-based approach to selectively sense Ag(I) was first disclosed by Ahn and co-workers in 2009.[54] Thus, the *N*-iodoethyl-rhodamine lactam **95** (Fig. 27) underwent the spirolactam ring-opening that was promoted by the coordination of Ag(I) to the iodide in EtOH/H_2O (20:80, v/v), producing the ring-opened product **95a**.

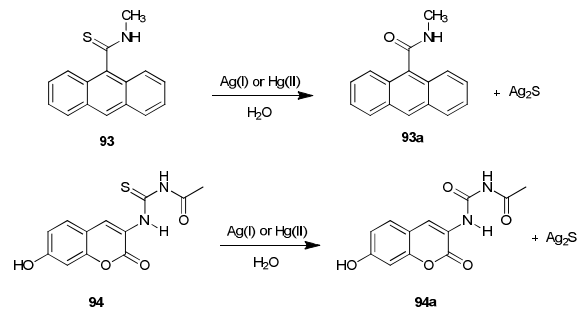

93 93a 94 94a

Fig. 26 Fluorescence sensing of Ag(I)/Hg(II) based on desulfurization of thioamide **93** and thiourea **94**.

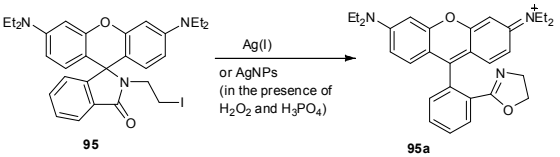

95 95a

Fig. 27 Structure of Ag(I)-selective reaction-based fluorescent chemosensor **95** and its reaction mechanism.

This chemical conversion was specific to Ag(I) among many metal ions examined, demonstrating the powerfulness of the reaction-based approach to realize a complete analyte selectivity. The conversion accompanied with a colour change from colourless to pink as well as a turn-on type fluorescence change with an orange emission band at 558 nm. The probe gave a good linear response toward Ag(I) in the concentration range of 0.1–5.0 μM, with the detection limit of 14 ppb. They further demonstrated that such a reaction-based probe can be used to detect AgNPs quantitatively for the first time, by combining the redox conversion of AgNPs to Ag(I) in the presence of H_2O_2 and phosphoric acid. The probe was applied for the simple quantification of AgNPs in consumer products such as a hand sanitizer gel and a fabric softener.

On the basis of the strong affinity of Ag(I) and Hg(II) ions toward selenium, Ma and co-workers developed the rhodamine B selenolactone **96** (Fig. 28) as a fluorescence probe for imaging of Ag(I) and Hg(II) in live cells.[189] The strong affinity of selenium towards silver and mercury accelerated the rhodamine ring-opening followed by hydrolysis of the seleno ester, releasing of the highly fluorescent rhodamine B (**96a**). Among the various metal ions, only Hg(II) or Ag(I) selectively turned-on the fluorescence (10-fold at 580 nm) in HEPES buffer (pH = 7.2) containing 0.5% 1,4-dioxane. The reaction was fast and nearly complete within 30 s, and the detection limits of 23 nM for Hg(II) and 52 nM for Ag(I) were obtained. Moreover, due to the higher affinity of selenium (Se) for Ag(I) than for Cl^-, the probe reacted with Ag(I) even in the presence of a high concentration of chloride. Hence the probe was applicable to imaging of cellular Ag(I), which is a challenging issue as the high cellular chloride concentration (more than mM levels) may lead to the precipitation of Ag(I) as AgCl to hinder the imaging of cellular Ag(I) in HeLa cells.

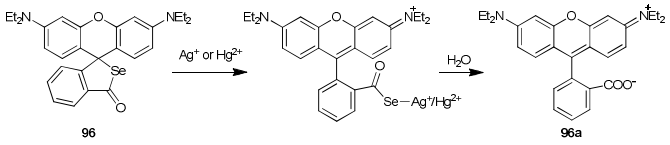

Fig. 28 Structure of the rhodamine B selenoacetone **96** and its reaction mechanism in presence of Ag(I) or Hg(II).

Wang and co-workers reported a simple sensing scheme for Ag(I) and Cu(II), which was based on the metal catalyzed oxidation of *o*-phenylenediamine (**97**) into the highly fluorescent 2,3-diaminophenazine **97a** (λ_{em} = 568 nm) (Fig. 29).[190] The reduction of Ag(I) or Cu(II) resulted in the formation of the corresponding metal nanoparticles, which, in turn, catalyzed the oxidation process. This autocatalytic sensing system allowed them to detect Ag(I) in the concentration range from 60 nM to 60 μM with a detection limit of 60 nM under optimal conditions. Furthermore, a paper sensor was developed using **97**, which was used to detect Ag(I) at levels as low as 0.06 nM with the detection ranges of 0.06–60 nM under the irradiation of UV light (365 nm). The response from Ag(I) or Cu(II) was shielded respectively by addition of chloride or ethylenediamine tetraacetic acid disodium salt, respectively.

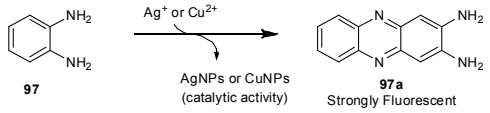

Fig. 29 Oxidation of *o*-phenylenediamine **97** in presence of Ag(I) or Cu(II).

3.2.3. Nanoparticle or macromolecular sensing systems

Attachment of receptor or reaction moieties onto a solid support produce "integrated" sensing systems containing multi or poly ligands. The integrated sensing systems, generally, exhibit enhanced sensing properties due to the cooperative effect through multi-binding or multi-reaction sites. Accordingly, integrated sensing systems for Ag(I) were developed based on oligonucleotides, quantum dots, nanoparticles, or polymers platforms.

3.2.3.1. Oligonucleotide-based sensing systems

Numerous sensing systems have been developed for Ag(I) in aqueous solution, based on organic fluorophores, quantum dots, nanoparticles and polymers (see below). However, many of these show low water-solubility, which would restrict their use for bioimaging purposes. In that respect, oligonucleotide-based sensing systems have been received significant attention.[191]

In 2008, Ono and co-workers first unexpectedly observed that Ag(I) stabilized DNA duplexes containing the naturally occurring cytosine–cytosine (C–C) mismatch-base pair through the C-Ag-C coordination (Fig 30a).[192] This observation has been widely adopted in the nanoparticle-based or macromolecular sensing systems in the following sections. Based on this unique binding mode, Ono and co-workers developed a DNA-based Ag(I) sensing system that employed an oligodeoxyribonucleotide (ODN) containing a C-rich part for the specific coordination involving Ag(I). The ODN-based sensing system consisted of a fluorescein dye (F) as the fluorophore and a dabcyl dye (D) as the quencher at the 3'- and 5'-ends, respectively (Fig. 30b). The ODN probe existed as a random coil in the absence of Ag(I), but become a hairpin structure in the presence of Ag(I) ions owing to the base pairing by the C–Ag(I)–C coordination. In the hairpin structure, the termini of the ODN are brought into close proximity, thereby enhancing the fluorescence resonance energy transfer (FRET) between the F and D moieties; as a result, the fluorescence was quenched, offering a novel detection means. Followed by the report of Ono and co-workers, several DNA- and oligonucleotide-based Ag(I) detection systems have been developed, mostly based on the selective C–Ag(I)–C pair formation.[193–204] Some selected examples are discussed here.

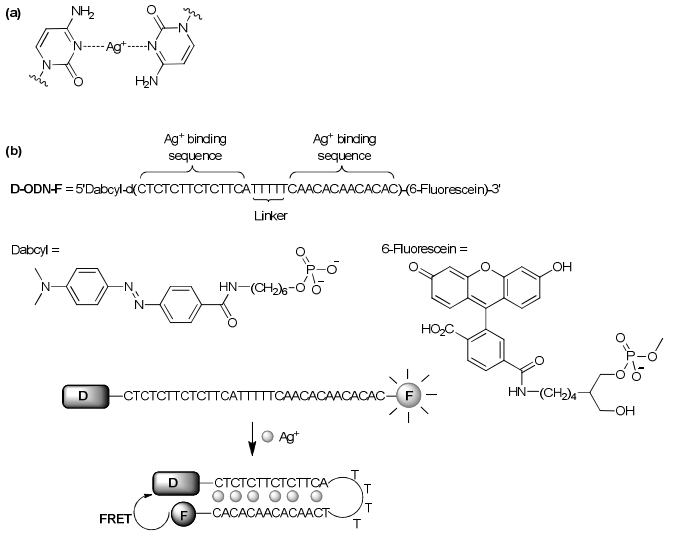

Fig. 30 (a) Selective binding mode of Ag(I) with cytosine (C) residue. (b) Structures of the ODN-based silver sensing system and a schematic representation of the hairpin structure induced by Ag(I) ions, which results in fluorescence quenching.

Tseng and co-workers reported that a double-strand-chelating dye, SYBR Green I (SG), exhibited weak fluorescence upon binding to single-stranded DNA (ssDNA), while it showed more than 11-fold fluorescence enhancement upon binding with Ag(I) through the cytosine residues (Fig. 31).[193]

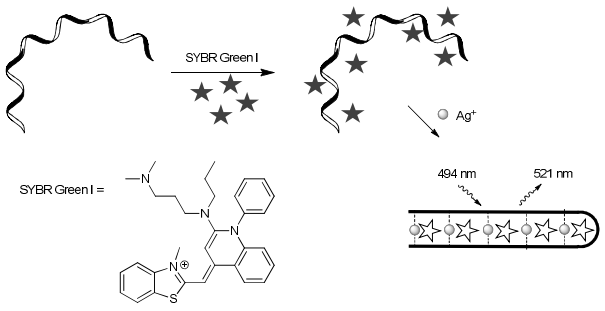

Fig. 31 Schematic representation of the Ag(I) detection method using SYBR Green I and a cytosine nucleotide (C-20).

A similar approach was also used by Yang *et al.* to develop a label-free fluorescence turn-on sensing system for Ag(I).[194]

Yang *et al.* reported that a nonemissive, aggregated complex between the cationic perylene fluorophore **98** (Fig. 32) and a C-rich ODN become fluorescent in the presence of Ag(I), enabling turn-on fluorescence sensing of the metal species.[195] The fluorescence change was explained by the C–Ag(I)–C coordination that induced a conformational change of the ODN into a hairpin structure which, in turn, led to the release of the dye molecules. Liu *et al.* reported that the AuNPs capped with the G-quadruplex (G4) units showed higher stability against salt-induced nanoparticle aggregation, and remained as mono-dispersed.[196] In contrast, upon addition of Ag(I), the G-quadruplex structure was unfolded, inducing aggregation of the AuNPs.

A different approach was reported by Kool and co-workers. They constructed a ODN-like oligomer that incorporated with fluorophores, the compound **99** (Fig. 32), which sensed Ag(I) with fluorescence enhancement.[205] The ODN mimic was identified through screening of a library of related compounds. Abasic spacers were incorporated on both ends of the oligomer to increase its aqueous solubility, prevent aggregation, and facilitate purification. The addition of Ag(I) to the ODN probe in buffer resulted in a new red-shifted emission band (at 720 nm) with an 8-fold fluorescence enhancement. The ODN probe showed high sensing ability even in chloride containing media, and thus used to imaging of Ag(I) in live HeLa cells.

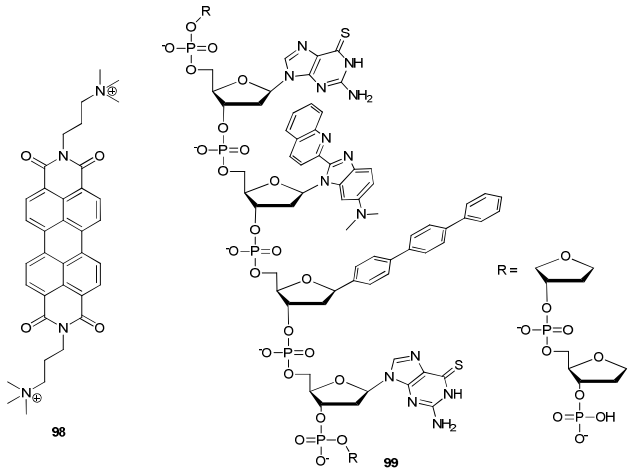

Fig. 32 Structures of the cationic perylene derivative **98** and the oligonucleotide mimic **99**.

3.2.3.2. Chemosensor based on quantum dots

Quantum dots are nanometer-sized luminescent semiconductor crystals that exhibit unique optical and electronic properties such as narrow, symmetric and stable fluorescence, along with size-dependent and tunable absorption and emission properties.[206,207] Compared with conventional organic fluorescent dyes, the use of quantum dots (QDs) for the detection of Ag(I) has advantageous features such as higher quantum yield (brighter), higher photostability, and higher photobleaching threshold (less blinking). Moreover, the functionalized QDs can be made water-soluble and biocompatible, which are important aspects for bioimaging application.

Quantum dot-based Ag(I) chemosensors have been mainly developed based on CdS, CdTe and CdSe quantum dots due to their specific interaction with and charge transfer property to Ag(I), which result in emission quenching.[208–217] The quantum dots were functionalized with various ligands to increase their water solubility, photophysical properties, and sensitivity towards Ag(I). Most of the sensing systems were developed based on the selective binding of Ag(I) with cytosine (C) nucleobases to form the C–Ag(I)–C type of a hairpin-like coordination complex (Fig. 30a).

Notably, Sun *et al.* constructed a label free, sensitive and selective luminescence sensing system for Ag(I), by combining CdTe QDs, $Ru(bpy)_2dppz^{2+}$, and cytosine (C)-rich single stranded DNA (C-ssDNA).[217] They prepared negatively-charged, water-soluble CdTe QDs, the surface of which was capped with thioglycolic acid (TGA). The QDs were further decorated with the positively Ru(II) complex (Fig. 33), which was nonemissive plausibly due to electron/energy transfer from the QD to the Ru(II) dye. Addition of C-ssDNA to the QDs removed the Ru(II) complexes on the QDs surface through electrostatic interactions, and the resulting "free" QDs emitted strongly. Upon addition of Ag(I) ions to the ensemble of QDs, Ru(II), and C-ssDNA, the fluorescence from the free QDs was quenched owing to the stronger binding of C-ssDNA with Ag(I) ions, which left behind the Ru(II) complexes and QDs that associate together to form the nonemissive Ru(II)-QD complexes.

Photoluminescent gold nanodots (AuNDs) on aluminum oxide nanoparticles (Al_2O_3 NPs) were also used for sensing Ag(I) through fluorescence quenching of AuNDs by metallophilic Ag(I)–Au(I) interactions.[218]

In 2013, Ran *et al.* reported a novel graphene quantum dots (GQDs) based system for rapid and label-free detection of Ag(I) with high sensitivity and selectivity.[219] Upon the attaching of Ag(I) on the surface of GQDs by electrostatic interaction, the fluorescence of GQDs at 420 nm was quenched due to charge transfer processes and consequently Ag(I) ions were reduced to generate AgNPs.

Compared with other metal ions, Ag(I) had much higher influence on the fluorescence quenching of GQDs because of the low reduction potential of Ag(I)/Ag. The reported method is simple in design and economic in operation, which offers a ''mix-and-detect'' protocol without dye-modified oligonucleotide or chemical modification of GQDs. Importantly, this strategy eliminates the need to use organic dyes, inorganic QDs and other toxic reagents.

Although the most of the quantum dot-based chemosensors exhibited high sensitivity towards Ag(I), but their quenching behaviour in presence of Ag(I) restricted their use for broad purposes. Moreover, some of them showed lack of selectivity due to interferences from competing heavy transition metal ions.

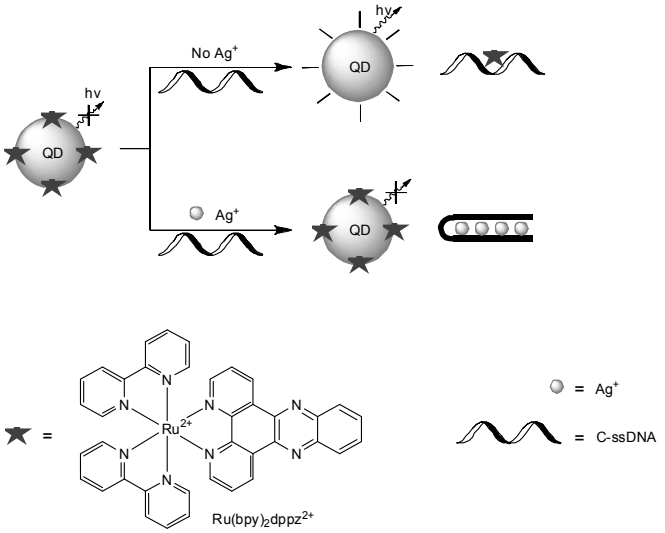

Fig. 33 Schematic diagram of fluorescence detection of Ag(I) based on light switching Ru-complex and QDs.

Accordingly, a few quantum dot-based sensing system that showed Ag(I)-specific enhanced emission was also reported. In 2005, Zhu and co-workers reported that CdS quantum dots (QDs) modified with L-cysteine detected Ag(I) through characteristic fluorescence enhancement with a gradual red-shift from 545 nm to 558 nm.[220] Wang and co-workers reported CdS NPs functionalized with mercaptoacetic acid that sensed Ag(I) in the fluorescence enhancement mode.[221] Compared with several fluorescence methods, the proposed method sensed Ag(I) in a wider linear range (from 0.08 nM to 0.15 nM) and with improved sensitivity (detection limit of 40 pM). Han and co-workers also reported CdTe QDs capped with thioglycolic acid (TGA) that selectively sensed Ag(I) in aqueous media, with a red-shift in the emission band (from 530 nm to longer wavelength).[222] In 2011, Wang and co-workers reported the first Ag(I)-selective fluorescent film sensor by doping CdS nanoparticles into polyurethane film.[223]

Recently, a cysteamine-capped CdS QDs for selective fluorescence sensing of Ag(I) and AgNPs in the fluorescence enhancement mode was also reported.[224] The sensing system was used to detect free Ag(I) in a solution of silver nanoparticles with high accuracy.

3.2.3.3. Chemosensors based on nanoparticles

Nanoparticle-based sensing systems have been employed for Ag(I) sensing in both ways, colorimetric and fluorescent methods. The colorimetric Ag(I) sensing systems are mainly based on the unique aggregation-induced colour change of gold nanoparticles (AuNPs) owing to the surface plasmon resonance (SPR) change.[225]

The AuNPs are usually modified with a specific ligand to stabilize them in solution as well as to provide them with specific binding selectivity towards Ag(I) in such a way to cause the aggregation of nanoparticles.[226–228] Notably, Tseng and co-workers reported the citrate-capped AuNPs modified with tween-20 that sensed Ag(I) and AgNPs with a minimum detectable concentration of 1 pM through nanoparticles aggregation.[226] But, the sensing system also provided a colorimetric change towards Hg(II).

Recently, Alizadeh and co-workers reported a AuNP-based colorimetric sensing system that sensed Ag(I) in an aqueous solution.[227] The AuNPs capped with 2-aminopyridine groups aggregated upon addition of Ag(I) ions by inter-nanoparticle coordination through the "pyridine-Ag(I)-pyridine" coordination, yielding a colour change from purple to blue. They also observed that the presence of silver benzoate increased the rate of complexation, which was explained by a different binding mode where Ag(I) was tri-coordinated involving an additional coordination to the carboxylate (Fig. 34).

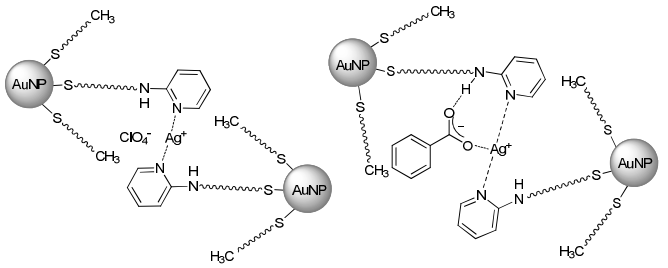

Fig. 34 Proposed coordination modes for the AuNPs capped with 2-aminopyridine groups in the absence and presence of silver benzoate.

Nanocrystals of fluorescent organic dyes were used to develop fluorescence sensing systems for Ag(I), as such molecular nanocrystals' fluorescence was quenched[229] or enhanced[230] upon interaction with the metal ions.

Fluorescent gold nanoclusters (AuNCs) also have been used as the sensing platform, as demonstrated by Yue *et al.* who reported protein-protected AuNCs[231] that responded to Ag(I) with a large blue-shifted and enhanced fluorescence.

Based on the formation of C–Ag(I)–C coordination, Li and co-workers developed DNA-functionalized gold nanoparticles which provided Ag(I) induced turn-on light-scattering switch.[232]

Ensemble sensing systems were also developed for fluorescence sensing of Ag(I).[233–235] Sun and co-workers reported that a ssDNA labeled with a fluorescent dye become quenched when it was adsorbed onto nano-C_{60}, but become emissive upon addition of Ag(I) ions.[233]

The C–Ag(I)–C coordination induced the ssDNA to fold into a hairpin structure and to be detached from the fluorescence-quenching nano-C_{60}, restoring the dye's fluorescence (Fig. 35). Using a similar sensing strategy, they also demonstrated the first use of carbon nanoparticles (CNPs), as another effective fluorescent sensing platform, for the selective detection of Ag(I) with a detection limit as low as 0.5 nM.[234]

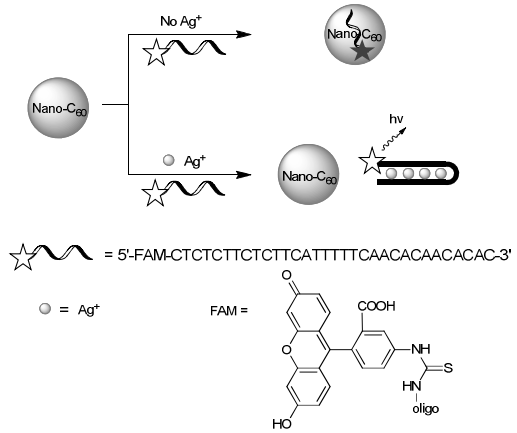

Fig. 35 Schematic diagram of fluorescence detection of Ag(I) based on C-rich ssDNA and nano-C_{60}.

Recently, Duan and co-workers reported a new strategy for the amplified detection of Ag(I) in aqueous solutions using nano-graphite-DNA hybrid and DNase I.[235] Nano-graphite quenched the fluorescence of dye-labelled C-rich ssDNA through strong π–π stacking interactions. Upon addition of Ag(I), the C–Ag(I)–C coordination induced the ssDNA to fold into a hairpin structure and to be detached from the surface of nano-graphite, which restored the dye's fluorescence (Fig. 36).

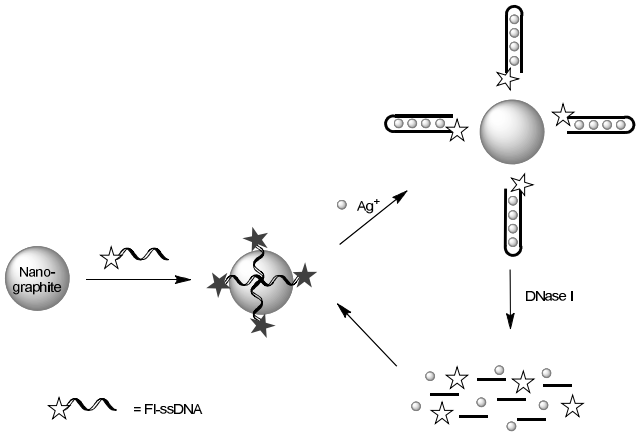

Fig. 36 Schematic illustration of the nanographite–ssDNA–DNase I sensing system for Ag(I).

Again the hairpin structure was cleaved by DNase I to release Ag(I) ions from the complex and bound with other dye-labelled ssDNAs on the nano-graphite surface. The successive release of dye-labelled ssDNAs from the nano-graphite resulted in significant signal amplification. By taking advantage of the super-fluorescence quenching efficiency of nano-graphite and DNase I amplification strategy, the biosensing system was able to detect Ag(I) down to 0.3 nM. Also, the high specificity of the C–Ag(I)–C coordination led to high selectivity to Ag(I) among other competing metal ions.

3.2.3.4. Polymer-based sensing systems

The detection of Ag(I) using polymer-based sensing systems was first demonstrated by Tong *et al.*[236] Thus, the conjugated polyquinolines **100** (Fig. 37) yielded interpolymer aggregates induced by Ag(I), which led to amplified fluorescence quenching (62-fold). The monomeric quinoline **100a** showed only 15-fold decrease in the fluorescence. The polymer system exhibited a high selectivity for Ag(I) over most of metal ions including Hg(II) and Pb(II). The reversibility of the sensing system was also observed: addition of several droplets of aqueous ammonia to a mixed solution Ag(I) and **100** in THF recovered the fluorescence of **100** (at 415 nm).

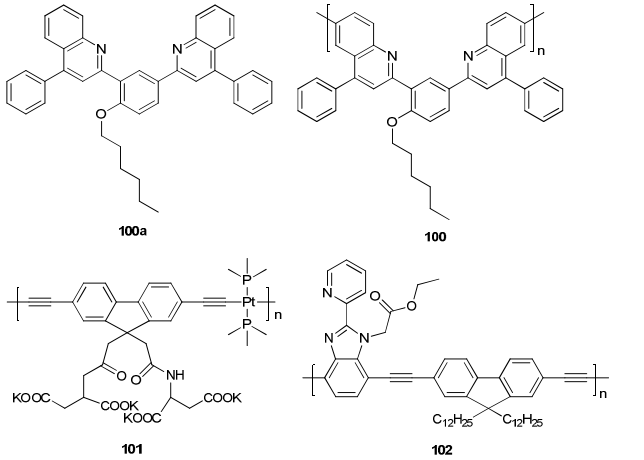

Fig. 37 Structures of polymer based sensing systems, **100–102**, and a monomer **100a.**

Qin *et al.* reported the conjugated polymer **101** that consisted of a platinum(II)-acetylide unit as a colorimetric sensing system for Ag(I) (Fig. 37).[237] A color change from colorless to yellow upon exposure of **101** to Ag(I) ions was observed, along with quenching of the fluorescence, which was explained due to the Ag(I)-induced intersystem crossing from the singlet to triplet states. Later, Wang *et al.* used an ensemble system consisted of a cationic polymer, ssDNA and AuNPs, which resulted in the aggregation of the nanoparticles through the C-Ag(I)-C coordination in the presence of Ag(I).[238]

Recently, Cao and co-workers reported the conjugated polymer **102** (Fig. 37) containing fluorene and ethyl 2-(2-(pyridin-2-yl)-1*H*-benzo[*d*]imidazol-1-yl)acetate (PBMA), which sensed Ag(I) with high sensitivity and selectivity.[239] Upon addition of Ag(I), the fluorescent emission from the polymer solution in THF was quenched dramatically, accompanying the color change from blue to green. The detection limit for Ag(I) was 50 nM.

The strong affinity of Ag(I) towards adenosine has also been exploited for the development of a coordination polymer system for sensing of Ag(I), as demonstrated by Chen and co-workers (Fig. 38).[240] Adenosine monophosphate (AMP) and Tb(III) were selected to construct the coordination polymer. The nucleobase moiety and phosphate group of AMP can serve as bi-dentate ligand of Tb(III).

The AMP–Tb(III) coordination polymer showed enhanced lanthanide fluorescence upon addition of Ag(I) ions, plausibly

due to the additional binding between the adenine base and the metal ion. A detection limit of 60 nM was obtained.

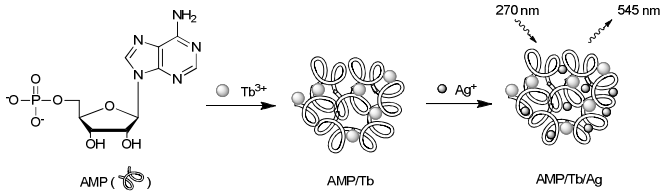

Fig. 38 Schematic illustration of the fluorescence enhancement of AMP/Tb by Ag(I).

The sensing characteristic of Ag(I)-sensing systems **24**–**97** are summarized in Tables 3–8 classified by the type of molecular structures and sensing mechanisms, which provide a quick overview on the selectivity, sensitivity, response time in some cases, bioimaging data, and basic experimental conditions and photophysical data. It is evident that biocompatible fluorescent sensing systems with bioimaging capability are still in great demand.

Also, it should be noted that most of the sensing systems are evaluated in media composed of high content of organic solvent, which preclude a direct comparison of their sensing properties because selectivity and sensitivity as well as emission properties are sensitive to the sensing environment.

Table 3 Sensing characteristics of compounds **24**–**37** containing cyclic *S*-donor ligands.

Compd.	Selectivity	Sensitivity, LOD[a]	Bioimaging data	Others	Ref
24	Ag(I), Hg(II), Cu(II)	▪ Up to ppb range in CH_3CN.	▪ Not reported	▪ Fluorescence enhancement only in CH_3CN towards Ag(I) (Φ = 0.22), Hg(II) (Φ = 0.59), Cu(II) (Φ = 0.25) ▪ In CH_3CN/H_2O (1:3, v/v), fluorescence enhancement towards Ag(I) (Φ = 0.24), Hg(II) (Φ = 0.58)	123
25	Ag(I), Hg(II)	▪ 1.2 ppm for Ag(I)	▪ Not reported	▪ In CH_3CN/H_2O (4:1, v/v) ▪ At 1.1 ppm metal concentration, selective only towards Ag(I) ▪ At 4.0 ppm metal concentration, selective towards Hg(II) and Ag(I)	124
26, **27**	Ag(I), Hg(II)	▪ Not reported	▪ Not reported	▪ In CH_3CN/H_2O (1:1, v/v) ▪ Ag(I): turn-on; Hg(II): turn-off	125
28	Ag(I)	▪ 0.1 μM ▪ Saturation: < 40 s	▪ Not reported	▪ In CH_3CN ▪ Turn-off type ▪ Used to develop fluorimetric optode membranes	126
29	Hg(II), Ag(I)	▪ 50 ppb for Hg(II)	▪ Imaging of HeLa cells incubated with Hg(II)	▪ In EtOH/Tris-HCl buffer (1:4, v/v, pH = 7.14) ▪ Hg(II): turn-on; Ag(I): turn-off ▪ Hg(II)-**29** complex: specific fluorescence response to Ag(I)	127
30	Ag(I), Hg(II)	▪ 0.01 μM for Ag(I)	▪ Not reported	▪ In CH_3CN/ HEPES buffer (1:1, v/v, pH = 7.4) ▪ Ag(I): 14-fold enhancement; Hg(II): 6-fold enhancement	128
31	Ag(I)	▪ 0.22 μM	▪ Not reported	▪ In EtOH/HEPES buffer (1:1, v/v, pH = 7.2) ▪ Turn-on type (150-fold) ▪ Stability constant for Ag(I)–**31** complex: log *K* = 10.2	129
32	Ag(I)	▪ 0.1 μM ▪ Saturation time: 2 min.	▪ Imaging of MCF-7 cells incubated with Ag(I)	▪ In HEPES buffer (pH = 7.4, 20 mM) containing $NaNO_3$ (100 mM) ▪ Turn-on type ▪ Efficient cell imaging (in cytoplasm and nucleolus)	130
33	Ag(I)	▪ Not reported	▪ Not reported	▪ In EtOH ▪ Ratiometric sensing mode (50 nm red-shift)	134
34–**36**	Ag(I), Hg(II)	▪ Not reported	▪ Not reported	▪ In CH_3CN ▪ Ratiometric sensing mode ▪ Fluorescence quantum yields in the order of **34**>**35**>**36**	135
37	Ag(I)	▪ Not reported	▪ Not reported	▪ In MES buffer (pH = 6.0) ▪ Ratiometric sensing mode (84 nm blue-shift) ▪ Ag(I)–**37** showed ratiometric sensing towards iodide	136

Table 4 Sensing characteristics of compounds **38**-**49** containing acyclic S-donor ligands.

Compd.	Selectivity	Sensitivity, LOD[a]	Bioimaging data	Others	Ref
38, **39**	Ag(I)	▪ Not reported	▪ Not reported	▪ In 1,4-dioxane/water (52:48, v/v) ▪ Turn-off type ▪ Stability constant: log K = 5.65 for Ag(I)–**38**; log K >7 for Ag(I)–**39**	137
40	Ag(I)	▪ Not reported	▪ Not reported	▪ In THF ▪ Ratiometric sensing mode	139
41	Ag(I)	▪ Not reported	▪ Not reported	▪ In HEPES buffer (50 mM, pH = 7.2) and 0.1 M KNO_3 ▪ Turn-on type (35-fold) ▪ Sensing is pH-independent	140
42	Ag(I)	▪ Not reported	▪ Not reported	▪ In CH_3CN ▪ Turn-off type ▪ Two-photon probe (δ = 1120 GM in CH_3CN, TP excitation wavelength = 810 nm)	143
43	Ag(I)	▪ Not reported	▪ Epithelial cells incubated with Ag(I)	▪ In CH_3CN ▪ Turn-off type ▪ Two-photon probe (δ = 950 GM in CH_3CN, TP excitation wavelength = 790 nm)	144
44	Ag(I)	▪ 0.8 μM	▪ Not reported	▪ In CH_3OH/HEPES buffer (3:1, v/v, pH = 7.0) ▪ Turn-on type (14-fold) ▪ Interference from Hg(II): 6-fold enhancement	145
45	Ag(I)	▪ 5 μM	▪ Not reported	▪ In MeOH/phosphate buffer (1:1, v/v, pH = 7.4) ▪ Turn-on type (with 44 nm red-shift) ▪ Enhanced ICT due to Ag(I) binding	146
46	Ag(I)	▪ 0.29 μM .	▪ Not reported	▪ In EtOH/HEPES (4:1, v/v, pH = 6.5) ▪ Turn-on type (60-fold) ▪ Restriction of C=N bond reorganization upon metal chelation	147
47	Ag(I)	▪ Not reported	▪ Not reported	▪ In DMSO/HEPES buffer (5:95, v/v, pH = 7.4) ▪ Turn-off type ▪ Color change from a light yellow to pink	148
48	Ag(I)	▪ 0. 2797 μM	▪ Not reported	▪ In EtOH/HEPES buffer (1:9, v/v, pH = 7.4) ▪ Turn-on type (PET blocking and the C=N bond isomerization) ▪ Color change from yellow to colorless	149
49	Ag(I)	▪ 0.35 ppb	▪ Not reported	▪ In MES buffer ▪ Turn-on type (Tb(III) luminescence) ▪ Supramolecular Ag(I) sensing system	150

Table 5 Sensing characteristics of compounds **50**-**76** containing non-S-donor ligands

Compd.	Selectivity	Sensitivity, LOD[a]	Bioimaging data	Others	Ref
50	Ag(I), Cu(II)	▪ Not reported	▪ Not reported	▪ In $CHCl_3$/EtOH (7:3, v/v) ▪ 0.3-fold fluorescence decrease	151
51	Ag(I)	▪ Not reported	▪ Not reported	▪ In $CHCl_3$/EtOH (7:3, v/v) ▪ Turn-off type (20-fold) ▪ Binding through Ag(I)-π interaction	151
52–**56**	Ag(I)	▪ 3 μM (for **52**), 8 μM (for **54**), 0.292 μM (for **55**), 0.65 μM (for **56**)	▪ Not reported	▪ Turn-off type ▪ Heavy metal ion effect (for **52** and **54**); reduced ICT (for **53**, **55**, and **56**) ▪ For **53**: strong quenching with Cu(II) also	152–155
57, **58**	Ag(I)	▪ Not reported	▪ Not reported	▪ In EtOH ▪ Turn-on type ▪ Cooperative binding interactions: Ag^+–K^+ (for **57**), and Ag^+–Cs^+ pairs (for **58**)	156
59	Ag(I)	▪ Not reported	▪ HeLa cells incubated with Ag(I)	▪ In EtOH/Tris buffer (4:6, v/v, pH = 7.5) ▪ Turn-on type (13-fold) type ▪ Binding mode was established	157
60	Ag(I)	▪ 0.052 μM	▪ Not reported	▪ In EtOH/H_2O (1:1, v/v) ▪ 4-fold fluorescence enhancement ▪ Binding based on selenophilicity of Ag(I)	158
61	Ag(I)	▪ Not reported	▪ Not reported	▪ In CH_3OH ▪ Turn-on type (Tb(III) luminescence)	159
62	Ag(I)	▪ Not reported	▪ Not reported	▪ In CH_3CN/HEPES buffer (8:2, v/v, pH = 6.2) ▪ 4-fold fluorescence enhancement	160
63, **64**	Ag(I)	▪ Not reported	▪ Not reported	▪ In THF ▪ Turn-on type (ca. 400-fold)	161

				▪ Enhanced ICT upon metal binding	
65	Cu(II), Ag(I)	▪ Not reported	▪ Not reported	▪ In CH_3CN/Tris buffer (3:7, v/v, pH = 7.0) ▪ "On-off-on" type ▪ Only ligand emission was quenched with Cu(II); ligand–Cu(II) complex's emission was enhanced with Ag(I)	[162]
66, **67**	Ag(I)	▪ 1.7 μM (for **66**)	▪ Hep-G2 cells incubated with Ag(I) using **66**	▪ In CH_3OH/H_2O (1:4, v/v) ▪ Turn-on type	[163]
68	Ag(I)	▪ Not reported	▪ Not reported	▪ In CH_3CN ▪ Turn-on type; Cu(II) and Hg(II) caused quenching ▪ Ag(I)–π interaction	[164]
69	Ag(I)	▪ 1.0 μM	▪ Not reported	▪ In DMSO ▪ Turn-on type (18-fold) ▪ Ag(I)-π interaction	[165]
70, **71**	Ag(I)	▪ 65.6 nM (for **70)**	▪ Not reported	▪ In MeOH/HEPES buffer (1:1, v/v, pH = 7.4) ▪ Ratiometric sensing mode (red shift: 30 nm for **70;** 10 nm for **71**) ▪ Ag(I)-arene interaction was established by X-ray crystallography	[166]
72	Ag(I)	▪ 0.34 μM	▪ Not reported	▪ In THF/H_2O (1:5, v/v) ▪ Turn-on type (AIE-based) ▪ Interference from Hg(II)	[167]
73	Ag(I)	▪ 0.2 μM	▪ Not reported	▪ In THF/H_2O (1:2, v/v) ▪ Ratiometric (AIE-based)	[168]
74	Ag(I), Cu(II), Hg(II)	▪ Not reported	▪ Not reported	▪ In CH_3OH ▪ Turn-off type and NIR emission ▪ Colour change from light reddish to purple	[169]
75	Ag(I)	▪ 34 nM (ca. 4 ppb)	▪ Not reported	▪ In MeOH/H_2O (1:4, v/v, pH = 5.4 succinic acid–NaOH buffer) ▪ Ratiometric and NIR emission	[170]
76	Ag(I)	▪ 0.2 μM	▪ Not reported	▪ In EtOH/HEPES buffer (1:40, v/v, pH = 7.0) ▪ Ratiometric and NIR emission	[171]

Table 6 Sensing characteristics of compounds **77**-**84** that show monomer-to-excimer conversion

Compd.	Selectivity	Sensitivity, LOD[a]	Bioimaging data	Others	Ref
77	Ag(I)	▪ Not reported	▪ Not reported	▪ In EtOH/H_2O (1:1, v/v, pH = 7.0) ▪ Ratiometric (I_{462}/I_{378}) ▪ 1:2 metal–ligand complexation	[173]
78	Ag(I)	▪ 0.1 μM	▪ Not reported	▪ In CH_3OH ▪ Ratiometric ▪ 2:1 metal–ligand complexation	[174]
79	Ag(I), AgNPs	▪ Not reported	▪ HeLa cells incubated with Ag(I)	▪ In HEPES buffer containing 1% of DMF or in HEPES buffer at pH 7.4 ▪ Ratiometric to Ag(I) (I_{480}/I_{380}) and to AgNPs (I_{500}/I_{378})	[175]
80	Ag(I)	▪ Not reported	▪ Not reported	▪ In THF ▪ Ratiometric (I_{478}/I_{395}) ▪ Adenine–Ag(I) complexation	[176]
81, **82**	Ag(I)	▪ Not reported	▪ Not reported	▪ In CH_3CN ▪ Cooperative binding-induced excimer formation with pinwheel systems ▪ Naphthyl fluorophore used (for **81)**	[177]
83	Ag(I)	▪ Not reported	▪ Not reported	▪ In CH_3CN/CH_2Cl_2 (1:1, v/v) ▪ Turn-on type (naphthyl excimer emission) ▪ Ag(I) and *N*-heterocyclic carbene coordination	[178]
84	Ag(I)	▪ Not reported	▪ Not reported	▪ Excimer between the pyridyl moieties ▪ Ratiometric (I_{445}/I_{315})	[179]

Table 7 Sensing characteristics of compounds **85**-**91** that show excimer-to-monomer conversion.

Compd.	Selectivity	Sensitivity, LOD[a]	Bioimaging data	Others	Ref
85	Ag(I)	▪ Not reported	▪ Not reported	▪ In MeOH/H_2O (200:1, v/v) ▪ Ratiometric (I_{374}/I_{484}) ▪ Hg(II) caused fluorescence quenching	[180]
86	Ag(I)	▪ Not reported	▪ Not reported	▪ In DMSO/HEPES buffer (1:1, v/v, pH = 7.4) ▪ Ratiometric (I_{463}/I_{399})	[181]

87	Ag(I)	▪ Not reported	▪ Not reported	▪ In EtOH/H_2O (9:1, v/v) ▪ Ratiometric (I_{377}/I_{470}) ▪ Fe^{3+} caused fluorescence quenching	[182]
88, **89**	Ag(I)	▪ Not reported	▪ Not reported	▪ In CH_3CN/CH_2Cl_2 (1000:1, v/v) ▪ Ratiometric ▪ Cu(II) and Hg(II) caused fluorescence quenching	[183]
90, **91**	Ag(I)	▪ Not reported	▪ Not reported	▪ In MeOH/$CHCl_3$ (98:2, v/v) ▪ Enhanced sensitivity for **90** than **91**	[184]

Table 8 Sensing characteristics of reaction-based sensing systems **92-97**.

Compd.	Selectivity	Sensitivity, LOD[a]	Bioimaging data	Others	Ref
92	Ag(I)	▪ 50 nM	▪ Not reported	▪ Colorimetric (colourless to blue), not fluorimetric ▪ Interference from Fe(III); solved by using chelating ligand ▪ *In situ* quantification of Ag(I) in the presence of AgNPs	[186, 187]
93	Hg(II), Ag(I)	▪ Not reported	▪ Not reported	▪ In HEPES buffer, pH = 7.0 ▪ Turn-on type (55-fold) ▪ Desulfurization-based	[85]
94	Hg(II), Ag(I)	▪ 2 ppb for Hg(II) and 1 ppb for Ag(I) ▪ Saturation: 2 min	▪ Not reported	▪ In a phosphate buffer (pH 7.0) containing 0.1% DMSO ▪ Turn-on type (400-fold)	[188]
95	Ag(I), AgNPs	▪ 14 ppb	▪ Not reported	▪ In EtOH/H_2O (1:4, v/v) ▪ Turn-on type ▪ Ag(I)–iodide coordination induced ring opening of a rhodamine spirolactam	[54]
96	Hg(II), Ag(I)	▪ 23 nM for Hg(II) and 52 nM for Ag(I)	▪ HeLa cells incubated with Ag(I)	▪ In HEPES buffer (pH = 7.2) containing 0.5% 1,4-dioxane ▪ Turn-on type (10-fold) ▪ Induced by selenofilicity of Hg (II) and Ag(I)	[189]
97	Ag(I), Cu(II)	▪ 60 nM for Ag(I) and 2.5 nM for Cu(II)	▪ Not reported	▪ A paper sensor was developed using **97**, which showed detection limit of 0.06 nM ▪ Metal-catalyzed oxidation of *o*-phenylenediamine	[190]

3.3. Summary and perspectives of silver detection

A variety of fluorescent sensing systems for Ag(I) species have been developed, spanning from small molecules to macromolecules and, furthermore, to quantum dots and nanoparticles.

The small-molecular sensing systems can be further classified into the coordination-based and the reaction-based ones, based on the sensing mode. The coordination-based Ag(I) sensing systems mostly rely on the strong affinity of Ag(I) to the soft sulfur donor, in addition to the nitrogen and oxygen donors in some cases. Also, the favourable coordination of Ag(I) to the π-electron-rich ligands such the carbon–carbon triple bond and aromatic rings has been exploited. The coordination of Ag(I) to the heteroatom-containing ligands leads to suppressed fluorescence in many cases, owing to the electron transfer between the fluorophore incorporated and the heavy transition metal ion. The coordination of Ag(I) to the alkyne or arene has been exploited to induce the excimer-to-monomer conversion of the arene fluorophore incorporated. Such coordination-based sensing systems can be forced to reversibly bind with Ag(I) by addition of a stronger ligand. On the other hand, the sensitivity of such coordination-based sensing systems is dependent on the association constant; hence, the limit of detection is not so low. Another inherent issue with the coordination-based sensing systems is the potential interference from other competing metal species, notably from Hg(I) as observed in many cases.

With respect to the sensitivity issue, the reaction-based sensing systems have been recognized to be a promising approach. Several notable sensing systems thus have been developed recently through incorporation of a Ag(I)-specific reactive group into a fluorophore in such a way that the chemical conversion causes fluorescence change. Although, most of the reported reaction based systems could show higher sensitivity, their selectivity towards Ag(I) was hampered by other competing metal ions. Only the Ag(I)-iodide interaction based system,[52] could overcame both the selectivity and sensitivity issue. Thus, the highly selective and sensitive reaction based sensing systems with promising features of molecular probes are yet to be developed for studying biological effects of Ag(I) species.

Along with the small-molecular based Ag(I) sensing systems, those based on the "integrated" or higher-order sensing platforms such as oligonucleotides, polymers, quantum dots, nanoparticles, and nanoclusters have received unusual attention from material scientists. Many of the integrated sensing systems are developed based on the unique molecular interaction between cytosine and Ag(I), as manifested in the

cytosine–Ag(I)–cytosine coordination in cytosine-rich oligonucleotides. Such higher-order sensing systems provide very low detection limits, even down to the picomolar level,[217,222] which is significantly lower than those (the sub-micromolar level) observed by the small-molecule based ones. Therefore, such integrated sensing systems can find their special usefulness where it is necessary to detect Ag(I) lower than the sub-micromolar range. Otherwise, the structural complexity casts several issues such as the availability, reproducibility, biocompatibility, etc., which would limit their applications, especially to biological systems. In this context, it should also be mentioned that many of the sensing systems, either small molecules or macromolecules, have been examined in organic media or in aqueous media containing high content of an organic solvent, which preclude the comparison of the selectivity and sensitivity data with those obtained in biocompatible aqueous media by other systems, because these properties are also dependent on the media.

Additionally, although some Ag(I) detection systems were applied for bioimaging application, it is still far away from reality. A possible reason is the high concentration of chloride ions inside cells, which precipitate out the silver ions as silver chloride and thus hampers the bioimaging. Further investigations to address this issue are demanded.

Also, in spite of many Ag(I) sensing systems, those for silver nanoparticles are quite limited although they are widely used in medical uses and consumer products for their antibacterial activities. Efficient sensing systems for silver nanoparticles and their applications to tackle biological effects of silver nanoparticles are still requisite.

Acknowledgements

We thank financial supports from the EPB center (R11-2008-052-01001) through the National Research Foundation and Ministry of Health & Welfare (HI13C1378), Korea.

Notes and references

[a] *Department of Chemistry and Center for Electro-Photo Behaviours in Advanced Molecular Systems, Pohang University of Science and Technology (POSTECH)77 Cheongam-Ro, Nam-Gu, Pohang, 790-784, Republic of Korea. Fax: (+82) 54-279-5877; E-mail: ahn@postech.ac.kr*

† Contributed equally to this work.

1) Z. Li, C. Brouwer and C. He, *Chem. Rev.*, 2008, **108**, 3239.
2) D. J. Gorin and F. D. Toste, *Nature,* 2007, **446**, 395.
3) A. Leyva-Perez and A. Corma, *Angew. Chem. Int. Ed.*, 2012, **51**, 614.
4) A. Corma, A. L. Pérez and M. J. Sabater, *Chem. Rev.*, 2011, **111**, 1657.
5) A. S. K. Hashmi, *Chem. Rev.*, 2007, **107**, 3180.
6) A. S. K. Hashmi and G. J. Hutchings, *Angew. Chem. Int. Ed.*, 2006, **45**, 7896.
7) A. Furstner and P. W. Davies, *Angew. Chem. Int. Ed.*, 2007, **46**, 3410.
8) J. H. Teles, S. Brode and M. Chabanas, *Angew. Chem. Int. Ed.*, 1998, **37**, 1415.
9) A. S. K. Hashmi, *Angew. Chem. Int. Ed.*, 2005, **44**, 6990.
10) M. Rudolph and A. S. K. Hashmi, *Chem. Soc. Rev.*, 2012, **41**, 2448.
11) W. E. Brenzovich Jr., *Angew. Chem. Int. Ed*., 2012, **51**, 8933.
12) R. Meyer, C. Lemire, S. K. Shaikhytdinov and H.-J. Freund, *Gold Bull*., 2004, **37**, 72.
13) R. Wilson, *Chem. Soc. Rev*., 2008, **37**, 2028.
14) S. L. Best and P. J. Sadler, *Gold Bull*., 1996, **29**, 87.
15) D. Krishnamurthy, M. R. Karver, E. Fiorillo, V. Orrú, S. M. Stanford, N. Bottini and A. M. Barrios, *J. Med. Chem*., 2008, **51**, 4790.
16) R. V. Parish and S. M. Cottrill, *Gold Bull*., 1987, **20**, 3.
17) R. Krikavova, J. Hosek, J. Vanco, J. Hutyra, Z. Dvorak, Z. travnicek, *Plos One*, 2014, **9**, e107373.
18) V. Milacic, D. Fregona and Q. P. Dou, *Histol. Histopathol.*, 2008, **23**, 101.
19) D. Wang and S. J. Lippard, *Nat. Rev. Drug Discov.*, 2005, **4**, 307.
20) A. S. Abu-Surrah and M. Kettunen, *Cur. Med. Chem.*, 2006, **13**, 1337.
21) W. D. Block and E. L. Knapp, *J. Pharmacol. Exp. Ther*., 1945, **83**, 275.
22) M.-T. Lee, T. Ahmed and M. E. Friedman, *J. Enzyme Inhib. Med. Chem*., 1989, **3**, 23.
23) J. R. E. Jones, *J. Exp. Biol*., 1940, **17**, 408.
24) E. Nyarko, T. Hara, D. J. Grab, A. Habib, Y. Kim, O. Nikolskaia, T. Fukuma and M. Tabata, *Chem. Biol. Interact*., 2004, **148**, 19.
25) A. J. Lewis and D. T. Walz, in *Progress in Medicinal Chemistry*, ed. G. P. Ellis and G. B. West, Elsevier Biomedical Press, Amsterdam, 1982, vol. 19.
26) S. P. Fricker, *Transit. Metal Chem*., 1996, **21**, 377.
27) P. Sinha, A. K. Wilson and M. A. Omary, *J. Am. Chem. Soc*., 2005, **127**, 12488.
28) L. A. Mullice, H. J. Mottram, A. J. Hallett and S. J. A. Pope, *Eur. J. Inorg. Chem*., 2012, 3054.
29) M. Osawa, I. Kawata, S. Igawa, A. Tsuboyama, D. Hashizume and M. Hoshino, *Eur. J. Inorg. Chem*., 2009, 3708.
30) M. Kriechbaum and U. Monkowius, *Annu. Rep. Prog. Chem., Sect. A: Inorg. Chem*., 2013, **109**, 188.
31) L. Rodríguez, C. Lodeiro, J. C. Lima and R. Crehuet, *Inorg. Chem.* 2008, **47**, 4952.
32) J. Arcau, V. Andermark, E. Aguiló, A. Gandioso, A. Moro, M. Cetina, J. C. Lima, K. Rissanen, I. Ott and L. Rodríguez, *Dalton Trans.*, 2014, **43**, 4426.
33) S. Marpu, Z. Hu and M. A. Omary, *Langmuir*, 2010, **26**, 15523.
34) E. E. Langdon-Jones and S. J. A. Pope, *Chem. Commun*., 2014, **50**, 10343.
35) J. Arcau, V. Andermark, E. Aguilo, A. Gandioso, A. Moro, M. Cetina, J. C. Lima, K. Rissanen, I. Ott and L. Rodriguez, *Dalton Trans*., 2014, **43**, 4426.
36) T. J. Robilotto, N. Deligonul, J. B. Updegraff III and T. G. Gray, *Inorg. Chem*., 2013, **52**, 9659.
37) C. P. Bagowski, Y. You, H. Scheffler, D. H. Vlecken, D. J. Schmitz and I. Ott, *Dalton Trans*., 2009, 10799.
38) A. Meyer, C. P. Bagowski, M. Kokoschka, M. Stefanopoulou, H. Alborzinia, S. Can, D. H. Vlecken, W. S. Sheldrick, S. Wölfl and I. Ott, *Angew. Chem. Int. Ed*., 2012, **51**, 8895.
39) R. G. Balasingham, C. F. Williams, H. J. Mottram, M. P. Coogan and S. J. A. Pope, *Organometallics*, 2012, **31**, 5835.

40) B. Bertrand and A. Casini, *Dalton Trans*., 2014, **43**, 4209.
41) H. B. Senturk, A. Gundogdu, V. N. Bulut, C. Duran, M. Soylak, L. Elci and M. Tufekci, *J. Hazard. Mater*., 2007, **149**, 317.
42) M. Soylak and M. Tuzen, *J. Hazard. Mater*., 2008, **152**, 656.
43) R. E. Sturgeon, C. L. Chakrabarti and C. H. Langford, *Anal. Chem*., 1976, **48**, 1792.
44) G. S. Reddi and C. R. M. Rao, *Analyst*, 1999, **124**, 1531.
45) R. Allabashi, W. Stach, A. de la Escosura-Muñiz, L. Liste-Calleja, A. Merkoçi, *J. Nanopart. Res.*, 2009, **11**, 2003.
46) A. Scheffer, C. Engelhard, M. Sperling, W. Buscher, *Anal. Bioanal. Chem.,* 2008, **390**, 249.
47) A. Ceresa, A. Radu, S. Peper, E. Bakker and E. Pretsch, *Anal. Chem*., 2002, **74**, 4027.
48) D. T. Quang and J. S. Kim, *Chem. Rev.,* 2010, **110**, 6280.
49) Y. Yang, Q. Zhao, W. Feng and F. Li, *Chem. Rev*., 2013, **113**, 192.
50) A. Gomes, E. Fernandes and J. L. F. C. Lima, *J. Biochem. Biophys. Methods*, 2005, **65**, 45.
51) Y.-K. Yang, S.-K. Ko, I. Shin and J. Tae, *Nat. Protoc.*, 2007, **2**, 1740.
52) X. Chen, T. Pradhan, F. Wang, J. S. Kim and J. Yoon, *Chem. Rev*., 2012, **112**, 1910.
53) M. Beija, C. A. M. Afonso and J. M. G. Martinho, *Chem. Soc. Rev*., 2009, **38**, 2410.
54) A. Chatterjee, M. Santra, N. Won, S. Kim, J. K. Kim, S. B. Kim and K. H. Ahn, *J. Am. Chem. Soc*., 2009, **131**, 2040.
55) M. J. Jou, X. Chen, K. M. K. Swamy, H. N. Kim, H.-J. Kim, S.-G. Lee and J. Yoon, *Chem. Commun*., 2009, 7218.
56) O. A. Egorova, H. Seo, A. Chatterjee and K. H. Ahn, *Org. Lett*., 2010, **12**, 401.
57) P. J. Sadler, *Gold Progress in Chemistry, Biochemistry and Technology*, ed. H. Schmidbaur, John Wiley & Sons, Chichester, 1999, pp 558.
58) Y.-K. Yang, S. Lee and J. Tae, *Org. Lett*., 2009, **11**, 5610.
59) Z. Li, C. Brouwer and C. He, *Chem. Rev*., 2008, **108**, 3239.
60) J. H. Do, H. N. Kim, J. Yoon, J. S. Kim and H.-J. Kim, *Org. Lett*., 2010, **12**, 932.
61) M. Dong, Y.-W. Wang and Y. Peng, *Org. Lett*., 2010, **12**, 5310.
62) J. Y. Choi, G.-H. Kim, Z. Guo, H. Y. Lee, K. M. K. Swamy, J. Pai, S. Shin, I. Shin and J. Yoon, *Biosens. Bioelectron.*, 2013, **49**, 438.
63) X. Cao, W. Lin and Y. Ding, *Chem. Eur. J*., 2011, **17**, 9066.
64) J.-B. Wang, Q.-Q. Wu, Y.-Z. Min, Y.-Z. Liu and Q.-H. Song, *Chem. Commun*., 2012, **48**, 744.
65) M. Emrullahoğlu, E. Karakuş, M. Üçüncü, *Analyst*, 2013, **138**, 3638.
66) B. Wang, T. Fu, S. Yang, J. Li and Y. Chen, *Anal. Methods*, 2013, **5**, 3639.
67) Z. R. Grabowski and K. Rotkiewicz, *Chem. Rev*., 2003, **103**, 3899.
68) H. Seo, M. E. Jun, O. A. Egorova, K.-H. Lee, K.-T. Kim and K. H. Ahn, *Org. Lett*., 2012, **14**, 5062.
69) O. A. Egorova, H. Seo, Y. Kim, D. Moon, Y. M. Rhee and K. H. Ahn, *Angew. Chem. Int. Ed*., 2011, **50**, 11446.
70) N. T. Patil, V. S. Shinde, M. S. Thakare, P. H. Kumar, P. R. Bangal, A. K. Barui and C. R. Patra, *Chem. Commun*., 2012, **48**, 11229.
71) L. Tian, Y. Yang, L. M. Wysocki, A. C. Arnold, A. Hu, B. Ravichandran, S. M. Sternson, L. L. Looger and L. D. Lavis, *Proc. Natl. Acad. Sci. U.S.A*., 2012, **109**, 4756.
72) H. Seo, M. E. Jun, K. Ranganathan, K.-H. Lee, K.-T. Kim, W. Lim, Y. M. Rhee and K. H. Ahn, *Org. Lett*., 2014, **16**, 1374.
73) L. Yuan, W. Lin, Y. Yang and J. Song, *Chem. Commun*., 2011, **47**, 4703.
74) S.-K. Ko, Y.-K. Yang, J. Tae and I. Shin, *J. Am. Chem. Soc*., 2006, **128**, 14150.
75) M. Üçüncü and M. Emrullahoğlu, *Chem. Commun*., 2014, **50**, 5884.
76) E. Karakuş, M. Üçüncü and M. Emrullahoğlu, Chem. Commun., 2014, **50**, 1119.
77) C. Rong, W. Jiliang, L. Hui, C. Gang, L. Zhong and C. Chi-Ming, *Rare Metals*, 2010, **29**, 180.
78) J. Xie, J. Y. Lee and D. I. C. Wang, *Chem. Mater.*, 2007, **19**, 2823.
79) B. K. Jena and C. R. Raj, *Langmuir*, 2007, **23**, 4064.
80) V. K. Kanuru, G. Kyriakou, S. K. Beaumont, A. C. Papageorgiou, D. J. Watson and R. M. Lambert, *J. Am. Chem. Soc*., 2010, **132**, 8081.
81) G. Kyriakou, S. K. Beaumont, S. M. Humphrey, C. Antonetti and R. M. Lambert, *ChemCatChem*., 2010, **2**, 1444.
82) J. Park, S. Choi, T.-I. Kim and Y. Kim, *Analyst*, 2012, **137**, 4411.
83) J. E. Park, M. G. Choi and S.-K. Chang, *Inorg. Chem*., 2012, **51**, 2880.
84) A. Corsaro and V. Pistará, *Tetrahedron*, 1998, **54**, 15027.
85) M.-Y. Chae and A. W. Czarnik, *J. Am. Chem. Soc*., 1992, **114**, 9704.
86) J. Wang, W. Lin, L. Yuan, J. Song and W. Gao, *Chem. Commun*., 2011, **47**, 12506.
87) Z. Öztaş, M. Pamuk and F. Algi, *Tetrahedron*, 2013, **69**, 2048.
88) P. Chinapang, V. Ruangpornvisuti, M. Sukwattanasinitt and P. Rashatasakhon, *Dyes Pigm.*, 2015, **112**, 236.
89) D. P. Murtha and R. A. Walton, *Inorg. Chem.*, 1973, **12**, 368.
90) T. J. Smith and R. A. Walton, *J. Inorg. Nucl. Chem.*, 1977, **39**, 1331.
91) *The Chemistry of Organic Derivatives of Gold and Silver*, ed. S. Patai and Z. Rappoport, John Wiley & Sons, Chichester, 1999.
92) M. Álvarez-Corral, M. Muñoz-Dorado and I. Rodríguez-Garcí, *Chem. Rev.*, 2008, **108**, 3174.
93) Y. Yamamoto, *Chem. Rev.*, 2008, **108**, 3199.
94) J.-M. Weibel, A. Blanc and P. Pale, *Chem. Rev.*, 2008, **108**, 3149.
95) S. Winstein and H. J. Lucas, *J. Am. Chem. Soc.*, 1938, **60**, 836.
96) J. P. Collman, L. S. Hegedus, J. R. Norton and R. G. Finke, in *Principles and Applications of Organotransition Metal Chemistry*, University Science Books, Mill Valley, 1987.
97) C. E. Willans, K. M. Anderson, P. C. Junk, L. J. Barbourc and J. W. Steed, *Chem. Commun.*, 2007, 3634.
98) W. Kirmse, *Carbene Chemistry*, Academic Press, New York, 2nd edn., 1971, vol. 1, pp. 85.
99) O. Guerret, S. Solé, H. Gornitzka, M. Teichert, G. Trinquier and G. Bertrand, *J. Am. Chem. Soc.*, 1997, **119**, 6668.
100) A. B. Lansdown, *Curr. Probl. Dermatol*., 2006, **33**, 17.
101) M. Yamanaka, K. Hara and J. Kudo, *Appl. Environ. Microbiol.*, 2005, **71**, 7589.
102) J. A. Lemire, J. J. Harrison and R. J. Turner, *Nat. Rev. Microbiol.*, 2013, **11**, 371.
103) R. M. Richards, R. B. Taylor and D. K. Xing, *J. Pharm. Sci.*, 1991, **80**, 861.
104) *Disinfection, Sterilization, and Preservation*, ed. S. S. Block, Lea & Febiger, Philadelphia, 3rd edn., 1983.

105) X.-B. Zhang, Z.-X. Hana, Z.-H. Fang, G.-L. Shen and R.-Q. Yu, *Anal. Chim. Acta*, 2006, **562**, 210.
106) S. Y. Liau, D. C. Read, W. J. Pugh, J. R. Furr and A. D. Russell, *Lett. Appl. Microbiol.*, 1997, **25**, 279.
107) K. B. Holt and A. J. Bard, *Biochemistry*, 2005, **44**, 13214.
108) Q. L. Feng, J. Wu, G. Q. Chen, F. Z. Cui, T. N. Kim and J. O. Kim, *J. Biomed. Mater. Res.*, 2000, **52**, 662.
109) M. K. Amini, M. Ghaedi, A. Rafia, I. Mohamadpoor-Baltork and K. Niknam, *Sens. Actuators B*, 2003, **96**, 669.
110) H. T. Ratte, *Environ. Toxicol. Chem.*, 1999, **18**, 89.
111) J. L. Barriada, A. D. Tappin, E. H. Evans and E. P. Achterberg, *Trends Anal. Chem.*, 2007, **26**, 809.
112) G. Yan, Y. Wang, X. He, K. Wang, J. Su, Z. Chen and Z. Qing, *Talanta*, 2012, **94**, 178.
113) Z. Szigeti, A. Malona, T. Vigassy, V. Csokai, A. Gŕun, K. Wygladacz, N. Ye, C. Xu, V. J. Chebny, I. Bitter, R. Rathore, E. Bakker and E. Pretsch, *Anal. Chim. Acta*, 2006, **572**, 1.
114) H. Yang, X. Liu, R. Fei and Y. Hu, *Talanta*, 2013, **116**, 548.
115) M. Hadioui, S. Leclerc and K. J. Wilkinson, *Talanta*, 2013, **105**, 15.
116) O. Heitzsch, K. Gloe, H. Stephan and E. Weber, *Solvent Extr. Ion Exch.*, 1994, **12**, 475.
117) R. K. Mahajan, I. Kaur, V. Sharma and M. Kumar, *Sensors*, 2002, **2**, 417.
118) R. A. Bell and J. R. Kramer, *Environ. Toxicol. Chem.*, 1999, **18**, 9.
119) H. E. Howard-Lock, *Met. Based Drugs.*, 1999, **6**, 201.
120) M. Oue, A. Ishigaki, Y. Matsui, K. Kimura and T. Shono, *J. Polym. Sci., Polym. Chem. Ed.,* 1985, **23**, 2033.
121) M. Oue, K. Kimura and T. Shono, *Analyst*, 1988, **113**, 551.
122) A. P. de Silva, *J. Phys. Chem. Lett.*, 2011, **2**, 2865.
123) K. Rurack, M. Kollmannsberger, U. Resch-Genger and J. Daub, *J. Am. Chem. Soc.*, 2000, **122**, 968.
124) G. Lin, H. Xu, Y. Cui, Z. Wang, Y. Yang and G. Qian, *Mater. Chem. Phys.*, 2013, **141**, 591.
125) M. Schmittel and H. Lin, *Inorg. Chem.*, 2007, **46**, 9139.
126) M. Shamsipur, K. Alizadeh, M. Hosseini, C. Caltagirone and V. Lippolis, *Sensor Actuat. B*, 2006, **113**, 892.
127) T. Chen, W. Zhu, Y. Xu, S. Zhang, X. Zhang and X. Qian, *Dalton Trans.*, 2010, **39**, 1316.
128) Z. Xu, S. Zheng, J. Yoon and D. R. Spring, *Analyst*, 2010, **135**, 2554.
129) C. S. Park, J. Y. Lee, E.-J. Kang, J.-E. Lee and S. S. Lee, *Tetrahedron Lett.*, 2009, **50**, 671.
130) M. Hu, J. Fan, J. Cao, K. Song, H. Zhang, S. Sun and X. Peng, *Analyst*, 2012, **137**, 2107.
131) A. Tamayo, E. Oliveira, B. Covelo, J. Casabó, L. Escriche and C. Lodeiro, *Z. Anorg. Allg. Chem.* 2007, **633**, 1809.
132) R. Y. Tsien and M. Poenie, *Trends Biochem. Sci.*, 1986, **11**, 450.
133) D. W. Domaille, L. Zeng and C. J. Chang, *J. Am. Chem. Soc.*, 2010, **132**, 1194.
134) H.-H. Wang, L. Xue, Y.-Y. Qian and H. Jiang, *Org. Lett.*, 2010, **12**, 292.
135) D. V. Berdnikova, Y. V. Fedorov and O. A. Fedorova, *Dyes Pigm.*, 2013, **96**, 287.
136) H. Wang, L. Xue and H. Jiang, *Org. Lett.*, 2011, **13**, 3844.
137) J. Ishikawa, H. Sakamoto, S. Nakao and H. Wada, *J. Org. Chem.*, 1999, **64**, 1913.
138) J. Ishikawa, H. Sakamoto and H. Wada, *J. Chem. Soc., Perkin Trans.*, 1999, **2**, 1273.
139) A. Coskun and E. U. Akkaya, *J. Am. Chem. Soc.*, 2005, **127**, 10464.
140) S. Iyoshi, M. Taki and Y. Yamamoto, *Inorg. Chem.*, 2008, **47**, 3946.
141) A. Rocha, M. M. B. Marques, C. Lodeiro, *Tetrahedron Lett*., 2009, **50**, 4930.
142) D. Kim, H. G. Ryu and K. H. Ahn, *Org. Biomol. Chem.*, 2014, **12**, 4550.
143) C. Huanga, X. Peng, Z. Lin, J. Fan, A Ren and D. Sun, *Sensor Actuat. B*, 2008, **133**,113.
144) C. Huanga, A. Ren, C. Feng and N. Yang, *Sensor Actuat. B*, 2010, **151**, 236.
145) H. Mu, R. Gong, L. Ren, C. Zhong, Y. Sun and E. Fu, *Spectrochim. Acta A*, 2008, **70**, 923.
146) V. Tharmaraj, S. Devi and K. Pitchumani, *Analyst*, 2012, **137**, 5320.
147) C. Yu, J. Zhang, M. Ding and L. Chen, *Anal. Methods*, 2012, **4**, 342.
148) K. M. K. Swamy, H. N. Kim, J. H. Soh, Y. Kim, S.-J. Kim and J. Yoon, *Chem. Commun.*, 2009, 1234.
149) T. Anand, G. Sivaraman, P. Anandh, D. Chellappa and S. Govindarajan, *Tetrahedron Lett.*, 2014, **55**, 671.
150) N. Iki, M. Ohta, T. Tanaka, T. Horiuchi and H. Hoshino, *New J. Chem.*, 2009, **33**, 23.
151) J. Kang, M. Choi, J. Y. Kwon, E. Y. Lee and J. Yoon, *J. Org. Chem.*, 2002, **67**, 4384.
152) Y. Zhou, H. Zhou, T. Ma, J. Zhang and J. Niu, *Spectrochim. Acta A*, 2012, **88**, 56.
153) L. Jia, Y. Zhang, X. Guoa and X. Qian, *Tetrahedron Lett.*, 2004, **45**, 3969.
154) J.-T. Hou, Q.-F. Zhang, B.-Y. Xu, Q.-S. Lu, Q. Liu, J. Zhang and X.-Q. Yu, *Tetrahedron Lett.*, 2011, **52**, 4927.
155) Y. Fu, L. Mu, X. Zeng, J.-L. Zhao, C. Redshaw, X.-L. Ni and T. Yamato, *Dalton Trans.*, 2013, **42**, 3552.
156) J. S. Kim, O. J. Shon, J. A. Rim, S. K. Kim and J. Yoon, *J. Org. Chem.*, 2002, **67**, 2348.
157) L. Xu, Y. Xu, W. Zhu, C. Yang, L. Han and X. Qian, *Dalton Trans.*, 2012, **41**, 7212.
158) S. Huang, S. He, Y. Lu, F. Wei, X. Zeng and L. Zhao, *Chem. Commun.,* 2011, **47**, 2408.
159) F. Dang, K. Lei and W. Liu, *J. Fluoresc.*, 2008, **18**, 149.
160) V. K. Bhardwaj, A. P. S. Pannu, N. Singh, M. S. Hundal and G. Hundal, *Tetrahedron*, 2008, **64**, 5384.
161) D. Ray, E. S. S. Iyer, K. K. Sadhu and P. K. Bharadwaj, *Dalton Trans.*, 2009, 5683.
162) R. Pandey, P. Kumar, A. K. Singh, M.Shahid, P.-z. Li, S. K. Singh, Q. Xu, A. Misra and D. S. Pandey, *Inorg. Chem.*, 2011, **50**, 3189.
163) D.-T. Shi, X.-L. Wei, Y. Sheng, Y. Zang, X.-P. He, J. Xie, G. Liu, Y. Tang, J. Li and G.-R. Chen, *Sci. Rep.*, 2014, **4**, 4252.
164) A. Azam, H. M. Chawla and S. Pandey, *Tetrahedron Lett.*, 2010, **51**, 4710.

165) Y.-P. Zhou, E.-B. Liu, J. Wang and H.-Y. Chao, *Inorg. Chem.*, 2013, **52**, 8629.
166) I. Takashima, A. Kanegae, M. Sugimoto and A. Ojida, *Inorg. Chem.*, 2014, **53**, 7080.
167) L. Liu, G. Zhang, J. Xiang, D. Zhang and D. Zhu, *Org. Lett.*, 2008, **10**, 4581.
168) J.-H. Ye, L. Duan, C. Yan, W. Zhang and W. He, *Tetrahedron Lett.*, 2012, **53**, 593.
169) X. Zhu, S. Fu, W.-K. Wong and W.-Y. Wong, *Tetrahedron Lett.*, 2008, **49**, 1843.
170) H. Zheng, M. Yan, X.-X. Fan, D. Sun, S.-Y. Yang, L.-J. Yang, J.-D. Li and Y.-B. Jiang, *Chem. Commun.*, 2012, **48**, 2243.
171) C.-Y. Li, X.-F. Kong, Y.-F. Li, C.-X. Zou, D. Liu and W.-G. Zhu, *Dyes Pigm.*, 2013, **99**, 903.
172) S. Nishizawa, Y. Kato and N. Teramae, *J. Am. Chem. Soc.*, 1999, **121**, 9463.
173) R.-H. Yang, W.-H. Chan, A. W. M. Lee, P.-F. Xia, H.-K. Zhang and K. A. Li, *J. Am. Chem. Soc.*, 2003, **125**, 2884.
174) B. Zhang, J. Sun, C. Bi, G. Yin, L. Pu, Y. Shi and L. Sheng, *New J. Chem.*, 2011, **35**, 849.
175) S. Jang, P. Thirupathi, L. N. Neupane, J. Seong, H. Lee, W. I. Lee and K.-H. Lee, *Org. Lett.*, 2012, **14**, 4746.
176) L. Liu, D. Zhang, G. Zhang, J. Xiang and D. Zhu, *Org. Lett.*, 2008, **10**, 2271.
177) J. Raker and T. E. Glass, *J. Org. Chem.*, 2001, **66**, 6505.
178) H. Zhang, L. Xie, W. Yan, C. He, X. Cao and C. Duan, *New J. Chem.*, 2009, **33**, 1478.
179) R. Joseph, B. Ramanujam, A. Acharya and C. P. Rao, *J. Org. Chem.*, 2009, **74**, 8181.
180) X. Liu, X. Yang, Y. Fu, C. Zhu and Y. Cheng, *Tetrahedron*, 2011, **67**, 3181.
181) F. Wang, R. Nandhakumar, J. H. Moon, K. M. Kim, J. Y. Lee and J. Yoon, *Inorg. Chem.*, 2011, **50**, 2240.
182) M. Kumar, R. Kumar and V. Bhalla, *Org. Lett.*, 2011, **13**, 366.
183) X.-L. Ni, X. Zeng, C. Redshaw and T. Yamato, *Tetrahedron*, 2011, **67**, 3248.
184) N.-J. Wang, C.-M. Sun and W.-S. Chung, *Sensor Actuat. B*, 2012, **171–172**, 984.
185) J. F. Zhang, Y. Zhou, J. Yoon and J. S. Kim, *Chem. Soc. Rev.*, 2011, **40**, 3416.
186) S. Liu, J. Tiana, L. Wang and X. Sun, *Sensor Actuat. B*, 2012, **165**, 44.
187) R. A. González-Fuenzalida, Y. Moliner-Martínez, M. González-Béjar, C. Molins-Legua, J. Verdú-Andres, J. Pérez-Prieto and P. Campins-Falco, *Anal. Chem.*, 2013, **85**, 10013.
188) K. Tsukamoto, Y. Shinohara, S. Iwasaki and H. Maeda, *Chem. Commun.*, 2011, **47**, 5073.
189) W. Shi, S. Sun, X. Li and H. Ma, *Inorg. Chem.*, 2010, **49**, 1206.
190) X. Yang and E. Wang, *Anal. Chem.*, 2011, **83**, 5005.
191) N. Dai and E. T. Kool, *Chem. Soc. Rev.*, 2011, **40**, 5756.
192) A. Ono, S. Cao, H. Togashi, M. Tashiro, T. Fujimoto, T. Machinami, S. Oda, Y. Miyake, I. Okamotoa and Y. Tanaka, *Chem. Commun.*, 2008, 4825.
193) Y.-H. Lina and W.-L. Tseng, *Chem. Commun.*, 2009, 6619.
194) Q. Yang, F. Li, Y. Huang, H. Xu, L. Tang, L. Wang and C. Fan, *Analyst*, 2013, **138**, 2057.
195) Y. Yang, W. Li, H. Qi, Q. Zhang, J. Chen, Y. Wang, B. Wang, S. Wang and C. Yu, *Anal. Biochem.*, 2012, **430**, 48.
196) G. Liu, Q. Zhang, Y. Qian, S. Yua and F. Li, *Anal. Methods*, 2013, **5**, 648.
197) T. Li, L. Shi, E. Wang and S. Dong, *Chem. Eur. J.*, 2009, **15**, 3347.
198) C. Zhao, K. Qu, Y. Song, C. Xu, J. Ren and X. Qu, *Chem. Eur. J.*, 2010, **16**, 8147.
199) Q. Xiao, S. Huang, Y. Ge, Z. He, Y. Liu and J. Liang, *J. Fluoresc.*, 2010, **20**, 541.
200) W. Pu, H. Zhao, C. Huang, L. Wu and D. Xua, *Microchim. Acta*, 2012, **177**, 137.
201) W. Y. Xie, W. T. Huang, N. B. Li and H. Q. Luo, *Chem. Commun.*, 2012, **48**, 82.
202) K. S. Park, J. Y. Lee and H. G. Park, *Chem. Commun.*, 2012, **48**, 4549.
203) G. Zhu, Y. Li and C.-y. Zhang, *Chem. Commun.*, 2014, **50**, 572.
204) L. Bian, X. Ji and W. Hu, *J. Agric. Food Chem.*, 2014, **62**, 4870.
205) S. S. Tan, Y. N. Teo and E. T. Kool, *Org. Lett.*, 2010, **12**, 4820.
206) H. Mattoussi, G. Palui and H. B. Na, *Adv. Drug Deliver. Rev.*, 2012, **64**, 138.
207) W. C. W. Chan, D. J Maxwell, X. Gao, R. E Bailey, M. Han and S. Nie, *Curr. Opin. Biotech.*, 2002, **13**, 40.
208) K. M. Gattás-Asfura and R. M. Leblanc, *Chem. Commun.*, 2003, 2684.
209) J.-H. Wang, H.-Q. Wang, H.-L. Zhang, X.-Q. Li, X.-F. Hua, Y.-C. Cao, Z.-L. Huang and Y.-D. Zhao, *Anal. Bioanal. Chem.*, 2007, **388**, 969.
210) J.-G. Liang, X.-P. Ai, Z.-K. He and D.-W. Pang, *Analyst*, 2004, **129**, 619.
211) A. Zheng, J. Chen, H. Li, C. He, G. Wu, Y. Zhang, H. Wei and G. Wu, *Microchim. Acta.*, 2009, **165**, 187.
212) R. Freeman, T. Finder and I. Willner, *Angew. Chem. Int. Ed.*, 2009, **48**, 7818.
213) B.-H. Zhang, L. Qi and F.-Y. Wu, *Microchim. Acta.*, 2010, **170**, 147.
214) P. P. Ingole, R. M. Abhyankar, B. L. V. Prasad and S. K. Haram, *Mater. Sci. Eng. B*, 2010, **168**, 60.
215) T.-T. Gan, Y.-J. Zhang, N.-J. Zhao, X. Xiao, G.-F. Yin, S.-H. Yu, H.-B. Wang, J.-B. Duan, C.-Y. Shi and W.-Q. Liu, *Spectrochim. Acta.*, *A* 2012, **99**, 62.
216) Y. Cao, A. Zhang, Q. Ma, N. Liu and P. Yang, *Luminescence*, 2013, **28**, 287.
217) W. Sun, J. Yao, T. Yao and S. Shi, *Analyst*, 2013, **138**, 421.
218) P.-C. Chen, T.-Y. Yeh, C.-M. Ou, C.-C. Shih and H.-T. Chang, *Nanoscale*, 2013, **5**, 4691.
219) X. Ran, H. Sun, F. Pu, J. Ren and X. Qu, *Chem. Commun.*, 2013, **49**, 1079.
220) J.-L. Chen and C.-Q. Zhu, *Anal. Chim. Acta*, 2005, **546**, 147.
221) L. Wang, A.-N. Liang, H.-Q. Chen, Y. Liu, B.-b. Qian and J. Fu, *Anal. Chim. Acta*, 2008, **616**, 170.
222) J. Wang, J. Liang, Z. Sheng and H. Han, *Microchim. Acta*, 2009, **167**, 281.
223) S. Wang, D. Yu, Y. Huang, J. Guo and Y. Wei, *Mater. Sci. Eng. B*, 2011, **176**, 271.
224) T. Khantawa, C. Boonmee, T. Tuntulani and W. Ngeontae, *Talanta*, 2013, **115**, 849.

225) M. E. Ali, U. Hashim, S. Mustafa, Y. B. C. Man and K. N. Islam, *J. Nanomater.*, 2012, Article ID 103607.
226) C.-Y. Lin, C.-J. Yu, Y.-H. Lin and W.-L. Tseng, *Anal. Chem.*, 2010, **82**, 6830.
227) A. Alizadeha, M. M. Khodaeia, Z. Hamidia and M. b. Shamsuddin, *Sensor Actuat. B*, 2014, **190**, 782.
228) G. D. Huy, M. Zhang, P. Zuo and B.-C. Ye, *Analyst*, 2011, **136**, 3289.
229) F. Qu, J. Liu, H. Yan, L. Peng and H. Li, *Tetrahedron Lett.*, 2008, **49**, 7438.
230) H. Yan, H. Su, D. Tian, F. Miao and H. Li, *Sensor Actuat. B*, 2011, **160**, 656.
231) Y. Yue, T.-Y. Liu, H.-W. Li, Z. Liu and Y. Wu, *Nanoscale*, 2012, **4**, 2251.
232) D.-Q. Feng, G. Liu, W. Zheng, J. Liu, T. Chen and D. Li, *Chem. Commun.*, 2011, **47**, 8557.
233) H. Li, J. Zhai and X. Sun, *Analyst*, 2011, **136**, 2040.
234) H. Li, J. Zhai and X. Sun, *Langmuir*, 2011, **27**, 4305.
235) Y. Wei, B. Li, X. Wang and Y. Duan, *Biosens. Bioelectron.*, 2014, **58**, 276.
236) H. Tong, L. Wang, X. Jing and F. Wang, *Macromolecules*, 2002, **35**, 7169.
237) C. Qin, W.-Y. Wong and L. Wang, *Macromolecules*, 2011, **44**, 483.
238) F. Wang, Y. Wu, S. Zhan, L. He, W. Zhi, X. Zhou and P. Zhou, *Aust. J. Chem.*, 2013, **66**, 113.
239) G. Xianga, W. Cuia, S. Lina, L. Wanga, H. Meierb, L. Li and D. Cao, *Sensor Actuat. B*, 2013, **186**, 741.
240) H. Tan and Y. Chen, *Chem. Commun.*, 2011, **47**, 12373.

Author information

Dr. Subhankar Singha received his B.S. in 2005 from Midnapore College, and M.S. in 2007 from Indian Institute of Technology (IIT), Kharagpur, India. He obtained his Ph.D. in Organic Chemistry from POSTECH, Republic of Korea, in 2013 under the supervision of Professor Kyo Han Ahn on the topic of "Studies on donor-acceptor type fluorophores and two-photon probes for bioimaging application". He is now working in the same group as post-doctoral researcher. His research interest is focused on the development of two-photon probes for small molecules associated with signal transductions.

Dr. Dokyoung Kim received his B.S. from the Department of Chemistry at Soongsil University in 2006 and his Ph.D. in Organic Chemistry from POSTECH in 2014 under supervision of Professor Kyo Han Ahn on the topic of "Development of two-photon absorbing materials and fluorescent probes for bio-imaging". He is now working in the University of California, San Diego under supervision of Professor Michael J. Sailor (2015-present), as post-doctoral researcher. His research interest is focused on the development of two-photon absorbing materials and organic/inorganic hybrid materials for investigating diseased-associated biological processes.

Dr. Hyewon Seo received her B.S. from the Department of Chemistry at Kyung Hee University in 2009 and her Ph.D. in Organic Chemistry from POSTECH in 2014 under supervision of Professor Kyo Han Ahn on the topic of "Development of reaction-based fluorescent probes for gold ions". She is now working in the Samsung SDI as researcher.

Seo Won Cho received her B.S. in 2013 from the Department of Chemistry at Chonnam National University. She is currently pursuing her Ph.D. study at the Department of Chemistry, POSTECH, under the supervision of Professor Kyo Han Ahn. She is working on the development of two-photon absorbing materials and their applications for bioimaging.

Professor Kyo Han Ahn received his B.S. from Seoul National University in 1980 and his Ph.D. in Organic Chemistry from KAIST in 1985 under supervision of Professor Sunggak Kim. After working for Yuhan pharmaceutical company shortly, he moved to the Department of Chemistry at POSTECH in 1986. He worked with Professor Kyriacos C. Nicolaou at University of Pennsylvania (1988), Professor Elias J. Corey at Harvard University (1995), and Professor Michael J. Sailor at University of California at San Diego (2002), as visiting scholar during his sabbatical leaves. His current research interests include luminescent materials, molecular probes and imaging agents, and bioconjugation.

Table of contents